UNIVERSIDADE DE LISBOA

FACULDADE DE CIÊNCIAS

DEPARTAMENTO DE QUÍMICA E BIOQUÍMICA

Deciphering parasite persistence in adipose tissue

Tiago Bizarra Rebelo

Mestrado em Bioquímica
Especialização em Bioquímica

Dissertação orientada por:
Luísa Miranda Figueiredo
Francisco Rodrigues Pinto

2017

ACKNOWLEDGEMENTS

Em primeiro lugar, muito obrigado Luísa! Obrigado por me aceitares no teu laboratório. Agradeço-te por todo o apoio e acompanhamento ao longo deste projeto. Superaste quaisquer expectativas (boas!) que tinha. Aprender contigo foi definitivamente um privilégio!

Obrigado Sandra! Por todos os teus ensinamentos, dedicação e paciência que tens para o teu estudantezinho. Sem a tua ajuda, este projeto não teria sido possível. Obrigado por me fazeres crescer enquanto cientista!

Merci Karine! You make the crazy world of immunology seem easier. Thank you for your dedication! A special thanks for the encouraging notes you left on the bench during the long long flow cytometry experiments. They made my day!

Gostaria de agradecer a todos os elementos do laboratório que de uma forma ou de outra contribuíram para a evolução do meu projeto, da minha carreira enquanto cientista e de como sou enquanto pessoa.

To Jess, for the friendship. For all the morning coffees, pleasant conversations and encouragement. Thank you for your fantastic book recommendations! I look forward to hear you speak Portuguese (just a little bit, please)!

Merci Fabien, le génie. Merci pour l'amitié. Pour me tenir compagnie pour le week-end. Et pour m'aider dans tout ce dont j'ai besoin. (Aproveita! É a tua única oportunidade para te rires do meu francês :D)

À Mariana, pela amizade! Ter uma parceira nesta luta torna tudo definitivamente mais fácil. E obrigado por toda a ajuda com os gráficos!

Ao Henrique, pela amizade e por todas as discussões imunológicas. Acima de tudo, muito obrigado por me teres ajudado na reta final da escrita da tese. Sem a tua contagem de parasitémias, não teria conseguido entregar a tempo!

À Margarida, por toda a preciosa ajuda ao longo deste ano! As minhas apresentações serão sempre mais bonitas agora porque está tudo alinhado!

Ao Miguel, obrigado pelo apoio e por me teres ajudado em tudo o que precisava! Bem que podias ter feito algum truque de magia para esta tese aparecer escrita…

Obrigado Leonor, por toda a ajuda! A tua maluqueira torna este laboratório num lugar único!

À Pena, por todo o apoio! E por esse riso contagiante!

Ao Idálio, muito obrigado por toda a ajuda e simpatia! Ainda não me esqueci do susto que me pregaste! Qualquer dia terei de me vingar.

Ao Daniel, por todo o apoio! A tua genialidade não tem fim!

À Alexandra, o membro mais recente! Tenho a certeza que o teu percurso correrá pelo melhor.

Gostaria também de agradecer aos vizinhos Prudêncios: Marta, Francisca, Patrícia, Filipa, Fontinha, Raquel e António. Obrigado por fazerem deste laboratório um local tão incrível para se trabalhar.

Aos elementos do Bruno Silva-Santos Lab por terem acolhido tão bem este parasita (eu!). Sem a vossa ajuda, principalmente a encontrar um anticorpo no meio de milhares, o meu projeto não teria sido possível.

A todos os amigos que tive a sorte de conhecer durante a faculdade. Vera, Inês, Miguel, Tiago, Sabino, Felgueiras, um muito obrigado! Um especial obrigado à Patrícia que me acompanhou ao longo de todo este percurso. Contigo tudo foi mais risonho! Não te livras de mim tão facilmente :)

Obrigado Rita, Carolina e Susana (princess!) por todo o apoio e por me iniciarem neste mundo da investigação! Obrigado ainda pelos conselhos que tanto beneficiaram as minhas decisões!

Obrigado triwizard champions! Soraia e Tats, a minha vida não seria a mesma sem a vossa amizade. Um muito obrigado por tudo! 

Mais recentemente, Joana, obrigado por todo o apoio!

Finalmente, gostaria de agradecer à minha fantástica família. Aos meus avós: Aurora, Guilhermina e José. Um muito obrigado por tudo! Aos meus tios: Manuela, Jaime, Carla e David. Obrigado por todo o apoio! Aos meus primos: Rafaela e Gonçalo. Obrigado!

Aos meus pais estarei eternamente grato. Nada disto seria possível sem os vossos esforços! O mérito deste trabalho, qualquer que seja, será tanto meu como vosso.

Um muito obrigado à minha irmã, Raquel, pelo apoio incondicional. Obrigado por todos os almoços e jantares que cozinhaste para mim durante a escrita! Espero algum dia poder retribuir. Adoro-te!

ABSTRACT

Trypanosoma brucei is an extracellular protozoan parasite that causes Human African Trypanosomiasis (HAT), also known as sleeping sickness. Throughout its life cycle, *T. brucei* alternates between an insect vector and a mammalian host. In the mammalian host, adipose tissue was recently discovered to constitute a main reservoir for the parasites. This discovery might challenge what we know regarding mechanisms of transmission, virulence and persistence in the host. In this project, our aim was to identify factors that benefit parasite tropism to adipose tissue, both from parasite and host.

In the parasite-oriented perspective, we investigated if the persistence of *T. brucei* in adipose tissue depends on metabolic adaptations that parasites undergo in the fat. For this, we targeted three pathways that we predict to be important for parasites in the fat: fatty acid β-oxidation, acetate production and oxidative phosphorylation. To do so, mice were infected with parasites deficient in three key enzymes theoretically involved in such pathways. In this work, we have identified a protein of the mitochondrial electron transport chain to be the most promising candidate required for persistence of *T. brucei* in adipose tissue. These results are consistent with the model that oxidative phosphorylation is important for parasites that reside in adipose tissue.

In the host-oriented perspective, we investigated if the persistence of *T. brucei* in adipose tissue depends on a permissive/attenuated local immune response by the host. We focused our analysis on immune cells known to be important for the immune response against *T. brucei* and for adipose tissue homeostasis. We characterized the dynamics of several important immune cells including macrophages, monocytes and neutrophils (myeloid cells) and different subsets of T cells and pro-inflammatory cytokines that participate in the control of *T. brucei* infection. We also assessed the frequency of immune modulators, including regulatory T cells and markers associated to exhausted/unresponsive effectors. Next, we used mouse mutants to test the importance of some of these host factors in parasite tropism. We identified several immune players that might favour *T. brucei* persistence in adipose tissue. The most promising are B cells, which is not totally surprising due to the importance of immunoglobulins in this parasitic infection.

Overall, this work paved the way to understand why *T. brucei* parasites persist in adipose tissue. Further work will be necessary to characterize the mechanism of a subset of these factors.

Keywords: *Trypanosoma brucei*, adipose tissue, energy metabolism, immune response.

RESUMO

A Tripanossomíase Humana Africana (THA), vulgarmente denominada doença do sono, é uma doença tropical negligenciada causada por *Trypanosoma brucei*, um parasita unicelular e extracelular. Esta doença é endémica da África subsariana, onde aproximadamente 70 milhões de pessoas estão em risco de a contrair. Na ausência de tratamento, a doença do sono é quase sempre letal sendo as terapias atualmente disponíveis difíceis de administrar, de elevada toxicidade e eficácia limitada.

Ao longo do seu ciclo de vida, *T. brucei* alterna entre o seu vetor, a mosca tsé-tsé, e o hospedeiro, um mamífero. Neste último, durante a picada da mosca, os parasitas são libertados na corrente sanguínea, proliferando e invadindo os espaços intersticiais de diversos órgãos. Numa fase tardia da doença, os parasitas invadem o cérebro, dando origem a disrupções do padrão do sono, que dão o nome à doença. Recentemente, o tecido adiposo foi descrito como sendo um reservatório principal de parasitas no hospedeiro. A descoberta de um novo reservatório no hospedeiro conduz a novas perspetivas no que respeita a mecanismos de transmissão, virulência e persistência no hospedeiro. Deste modo, o estudo dos parasitas no tecido adiposo torna-se imperativo para compreender a dinâmica de infeção. De forma a responder a esta necessidade, o objetivo do presente estudo foi analisar fatores do parasita e do hospedeiro que possam contribuir para este tropismo.

No que respeita ao parasita, analisou-se uma potencial adaptação do seu metabolismo energético. Comparativamente aos parasitas do sangue, os parasitas que residem no tecido adiposo são transcriptomicamente diferentes, revelando um aumento na expressão de enzimas da β-oxidação e ciclo dos ácidos dos tricarboxílicos (TCA). Além disso, os parasitas do tecido adiposo conseguem metabolizar ácidos gordos através da β-oxidação. Deste modo, partimos da hipótese de que *T. brucei* se acumula no tecido adiposo porque, através da β-oxidação, poderá utilizar os ácidos gordos secretados pelos adipócitos como uma fonte de carbono. Hipoteticamente, o acetil-CoA formado na β-oxidação alimentaria o TCA, formando NADH e $FADH_2$ que, por sua vez, levaria à formação de ATP por fosforilação oxidativa. Num cenário alternativo, o acetil-CoA seria convertido em acetato, levando à produção de ATP. De modo a testar se os parasitas se acumulam no tecido adiposo porque catabolizam ácidos gordos, infetaram-se ratinhos com parasitas deficientes em enzimas das três vias metabólicas referidas: β-oxidação, produção de acetato e fosforilação oxidativa. A acumulação de *T. brucei* no tecido adiposo gonadal foi determinada por PCR quantitativo de DNA genómico.

Em infeções com parasitas mutantes, em que teoricamente se bloqueou a β-oxidação e a produção de acetato, observou-se que a ausência destes genes não leva a uma menor acumulação no tecido adiposo, pelo que não desempenham um papel neste tropismo. A fosforilação oxidativa foi bloqueada pela depleção de genes que codificam para proteínas da cadeia respiratória. A ausência de um destes componentes levou a um decréscimo na acumulação de parasitas específico do tecido adiposo. Estes resultados revelam um potencial envolvimento da fosforilação oxidativa na adaptação e acumulação dos parasitas no tecido adiposo.

No que respeita ao hospedeiro, analisou-se a resposta imune local. Para tal, partimos da hipótese que o *T. brucei* se acumula no tecido adiposo porque a resposta imune poderá ser permissiva/atenuada. Para testar esta hipótese, começámos por uma abordagem mais abrangente caracterizando, por citometria de fluxo, a dinâmica de populações de células imunes relevantes para a resposta imunitária contra o parasita durante o processo de infeção de um ratinho.

As células mieloides, especialmente macrófagos, possuem um papel chave no controlo do crescimento do parasita, durante a infeção, fagocitando parasitas opsonizados e produzindo citocinas pró-inflamatórias. Neste estudo, observou-se que monócitos/macrófagos e neutrófilos são recrutados rapidamente para o tecido adiposo, durante a infeção.

As células T efetoras são essenciais para controlar a infeção por *T. brucei*, principalmente através da produção de citocinas. Neste estudo, observou-se que as células T efetoras se acumulam no tecido adiposo, sugerindo que não existe nenhuma restrição no recrutamento das mesmas, assim como na produção de algumas citocinas. O papel do interferão-γ durante uma infeção por *T. brucei* tem sido alvo de controvérsia, uma vez que foi descrito como essencial para o combate à infeção e também como estímulo de crescimento para o parasita. Neste estudo observou-se primeiramente que o interferão-γ não aparenta ter um efeito direto no crescimento do parasita, *in vitro*. Posteriormente, *in vivo*, confirmou-se não só que o interferão-γ não favorece a proliferação do parasita como também contribui para a sua eliminação, uma vez que, em ratinhos deficientes para a produção desta citocina, a eliminação do parasita é reduzida. Os resultados sugerem que, apesar de ter sido descrito como estímulo de crescimento, o interferão-γ não contribui para a acumulação e persistência de *T. brucei* no tecido adiposo.

As células T reguladoras são essenciais para diminuir a resposta inflamatória que, se prolongada, conduz a consequências nefastas para o hospedeiro. Além disso, estas células constituem uma importante população de células residentes no tecido adiposo que mantêm o ambiente anti-inflamatório. Neste estudo mostrou-se que as células T reguladoras se acumulam no tecido adiposo, durante a infeção, sugerindo que poderão atenuar a ação das células T efetoras.

A homeostasia da população de células T reguladoras residentes no tecido adiposo depende de células T γδ produtoras de interleucina-17. Deste modo, a resposta atenuante das células T reguladoras poderia ser um efeito indireto da população de células T γδ produtoras de interleucina-17. Neste estudo observou-se que tanto as células T γδ como a produção de interleucina-17 não contribuem para acumulação do parasita no tecido adiposo.

PD-1 é um recetor inibitório, também conhecido por *checkpoint* imunitário, que regula negativamente a ativação de células T, após reconhecimento do ligando PD-L1. Neste estudo observou-se que a proporção de células que expressam PD-1 e PD-L1 é maior no tecido adiposo, sugerindo que este poderá ser um ambiente imunossuprimido. No entanto, o bloqueio da ligação PD-1/PD-L1, *in vivo*, não levou a uma alteração na eliminação do parasita no tecido adiposo, sugerindo que esta proporção mais elevada não favorece a acumulação do parasita neste órgão.

Por fim, as imunoglobulinas M desempenham um papel fulcral no controlo da infeção, permitindo a eliminação do parasita mediada por anticorpos. De forma a determinar se as imunoglobulinas M são também responsáveis pela eliminação dos parasitas no tecido adiposo, infetaram-se ratinhos que apenas produzem imunoglobulinas M de baixa afinidade, estando ausentes os outros isotipos. Neste estudo observou-se que as imunoglobulinas M de baixa afinidade são suficientes para eliminar o parasita do sangue e de outros órgãos, mas não do tecido adiposo. Este resultado revela um potencial papel das células B, especialmente a ação limitada das imunoglobulinas M, na acumulação de *T. brucei* no tecido adiposo.

De um modo geral, este estudo revelou um potencial papel da adaptação do metabolismo energético na persistência de *T. brucei* no tecido adiposo bem como diversos potenciais intervenientes imunitários que poderão favorecer a sua acumulação, constituindo um ponto de partida para perceber qual a vantagem de *T. brucei* se acumular no tecido adiposo. Esta acumulação preferencial poderá não só ter consequências para a persistência no hospedeiro, mas também na transmissão para o vetor. Em última análise, este conhecimento será crítico para o desenvolvimento de novas estratégias terapêuticas que deverão focar-se não só na eliminação dos parasitas do sangue, mas também dos parasitas do tecido adiposo.

Palavras-chave: *Trypanosoma brucei*, tecido adiposo, metabolismo energético, resposta imunitária.

LIST OF FIGURES AND TABLES

LIST OF ABBREVIATIONS

AAT: Animal African Trypanosomiasis
AID: Activation-induced Cytidine Deaminase
APC: Antigen Presenting Cell
ASCT: Acetate:succinate CoA-transferase
AT: Adipose Tissue
ATF: *T. brucei* Adipose Tissue Form
ATP: Adenosine 5'-Triphosphate
BSD: Blasticidin Resistance Gene
BSF: *T. brucei* Bloodstream Form
BV: Brilliant Violet
cAMP: cyclic Adenosine Monophosphate
CD: Cluster of Differentiation
CNS: Central Nervous System
cRPMI: complete Roswell Park Memorial Institute medium
DC: Dendritic Cell
DHAP: Dihydroxyacetone Phosphate
DMEM: Dulbecco's Modified Eagle Medium
DNA: Deoxyribonucleic Acid
DNAse: Deoxyribonuclease
dpi: day post-infection
ELISA: Enzyme-Linked Immunosorbent Assay
FITC: Fluorescein Isothiocyanate
Foxp3: Forkhead box P3 transcription factor
FSC: Forward-Scatter
G3P: Glycerol 3-phosphate
gDNA: genomic DNA
GFP: Green Fluorescent Protein
GPI: Glycosylphosphatidylinositol
HAT: Human African Trypanosomiasis
HMI: Hirumi's Modified Iscove's Medium
IFN-γ: Interferon gamma
Ig: Immunoglobulin
IGC: Instituto Gulbenkian de Ciência
IL: Interleukin
iMM: Instituto de Medicina Molecular
i.p.: Intraperitoneal
i.v.: Intravenous
mVSG: membrane form of VSG
MyD88: Myeloid Differentiation Primary Response Gene 88
NET: Neutrophil Extracellular Trap
NMS: Normal Mouse Serum
PAC: Puromycin Resistance Gene
PAMP: Pathogen-associated Molecular Patterns
PBS: Phosphate-Buffered Saline
PCF: *T. brucei* Procyclic Form
PCR: Polymerase Chain Reaction
PD-1: Programmed Cell Death Protein 1
PD-L1: Programmed Death-Ligand 1
Pen-Strep: Penicillin Streptomycin
PLC: Phospholipase C
PMA: Phorbol 12-Myristate 13-Acetate
PPAR-γ: Peroxisome Proliferator Activated Receptor-gamma
PRR: Pattern Recognition Receptors
qPCR: quantitative Polymerase Chain Reaction
RAG2: Recombination Activating Gene 2
rDNA: ribossomal Deoxyribonucleic Acid
RNA: Ribonucleic Acid
SIF: Stumpy Inducible Factor
SSC: Side-Scatter
sVSG: soluble VSG
TbAdC: *T. brucei* Adenylate Cyclase
TCA: Tricarboxylic Acid
TCR: T-Cell Receptor
TFEα: Trifunctional Enzyme subunit alpha
TGF-β: Transforming Growth Factor beta
TLR: Toll-like Receptor
TLTF: Trypanosome Lymphocyte Triggering Factor
TNF-α: Tumor necrosis factor alpha
Treg: Regulatory T cell
UTR: Untranslated Region
VSG: Variant Surface Glycoprotein

TABLE OF CONTENTS

1. INTRODUCTION

1.1. Human and Animal African Trypanosomiasis

Trypanosoma brucei is an extracellular protozoan parasite that causes Human African Trypanosomiasis (HAT), also known as sleeping sickness. HAT belongs to the group of neglected tropical diseases with high social-economic impact in sub-Saharan Africa where approximately 70 million people were at risk of contracting the disease[1].

Two subspecies of *T. brucei* with indistinguishable morphologies are pathogenic to humans: *T. b. gambiense* and *T. b. rhodesiense*. Found in Western and Central Africa, *T. b. gambiense* causes the chronic form of the disease and accounts for more than 95% of the HAT reported cases. *T. b. rhodesiense*, found in Eastern and Southern Africa, is the agent responsible for the remaining 5% of the reported cases and causes an acute and fast-progressing infection[2].

The pathology of the disease is characterized by two stages. In the early haemolymphatic stage, parasites proliferate in the bloodstream and the lymphatic system, giving rise to non-specific symptoms such as fever, headache, weight loss, fatigue, arthralgia and malaise. As the disease progresses, patients may develop lymphadenopathy, hepatosplenomegaly, and cardiac and ophthalmological features[3]. The later meningo-encephalic stage is characterized by the invasion of the central nervous system (CNS) by the parasites. This leads to a wide spectrum of possible neurological features, including the characteristic sleep disturbances, which give the disease its name, as well as psychiatric and motor disorders[4]. If left untreated, sleeping sickness is lethal. Drug treatment is available, however current therapies hold difficulties in administration, toxicity and limited efficacy[5].

T. brucei, although to a lesser extent than *T. congolense* and *T. vivax*, is also a causative agent of Animal African Trypanosomiasis (AAT), which severely affects livestock and acts as a reservoir for the human parasites. Therefore, besides posing a major health concern, sleeping sickness also holds a great economic burden, limiting rural development. Domestic animals provide a source of steady income, in the form of milk, as well as a source of meat and draught power for agriculture. By infecting livestock and limiting such sources of income, it is estimated that 1.5 billion US dollars are lost annually[6]. Therefore, the major socio-economic impact of this disease and current treatment limitations justifies the need to study the mechanism of disease in infections caused by *T. brucei*.

1.2. The life cycle of *Trypanosoma brucei*

T. brucei transmission to a mammalian host occurs upon a bite of an infected tsetse fly (*Glossina spp*). During such blood meal, metacyclic forms, present in the salivary glands of the tsetse, are released into the bloodstream. This induces differentiation into long slender forms that proliferate and invade the interstitial spaces of many organs[3]. By a density-sensing mechanism, through which parasites release a still unknown stumpy induction factor (SIF), proliferating long slender forms differentiate into non-dividing short stumpy forms, which are infective to the insect vector[7]. When the vector bites the mammalian host, stumpy forms are ingested and undergo differentiation to procyclic forms (PCF) in the tsetse's midgut. Finally, proliferative PCF migrate to the salivary glands where they develop into quiescent metacyclic forms, which are pre-adapted for survival in a new mammalian host (**Figure 1**)[8].

In the mammalian host, four main reservoirs for *T. brucei* have been described: the blood and the brain, and more recently the adipose tissue (AT) and skin[9,10]. A study from our laboratory showed that parasites accumulate massively in AT, reaching levels roughly similar to the blood, and have a different gene expression signature than bloodstream forms (BSF)[9]. The presence of adipose tissue forms (ATF)

suggests a greater phenotypic variety of parasites within the mammalian host than previously anticipated. Furthermore, another recent study revealed parasite tropism to the skin of both mice and humans, in which parasites were observed to be in contact with subcutaneous adipocytes[10]. This accumulation may confer a selective advantage for *T. brucei* as the skin is the place for transmission. Overall, the presence of parasites in AT, of which the purpose remains elusive, brings new perspectives regarding drug treatment and infection dynamics, as most of what is known today was studied in BSF.

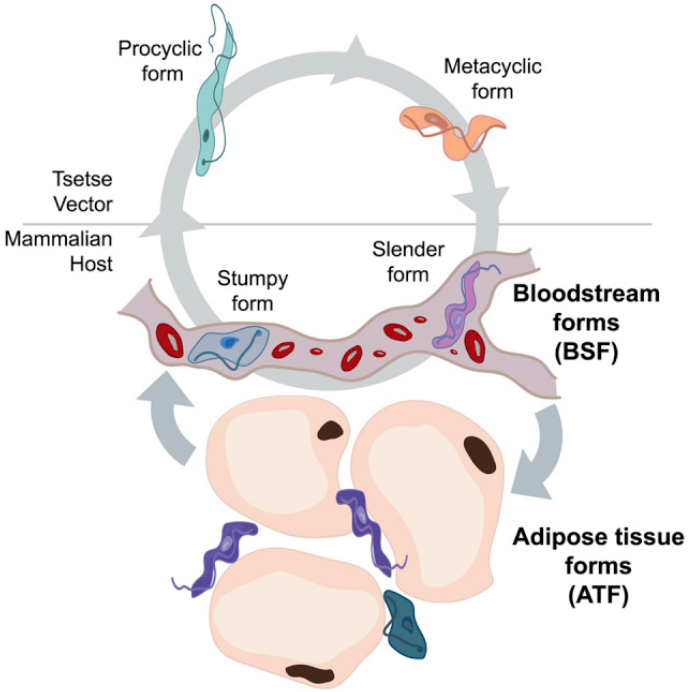

Figure 1. *T. brucei* life cycle. During its life cycle, *T. brucei* parasites alternate between an insect vector, tsetse fly, and a mammalian host. The different forms of the parasites are the result of developmental modifications that allow them to proliferate (procyclic forms, in the vector, and slender forms, in the host) and to pre-adapt for the next transmission event (metacyclic forms, in the vector, and stumpy forms, in the host). Within the mammalian host, parasites can also accumulate and persist in the adipose tissue, thus called adipose tissue forms. Adapted from 9.

1.3. Energy metabolism in *Trypanosoma brucei*

To complete its life cycle, *T. brucei* needs to alternate between an insect vector and a mammalian host, coming across distinct environments in terms of quantity and type of available nutrients as well as availability of oxygen. Thus, during its life cycle, parasites go through morphologic and metabolic changes to adapt to the new environmental conditions[11].

- **Bloodstream forms**

In the mammalian host, ATP production in slender BSF relies exclusively on glycolysis, through the conversion of glucose into pyruvate as the sole end-product. As blood provides a constant and glucose-rich environment, parasites proliferate at a high rate while producing all necessary ATP by aerobic glycolysis. Under low levels of oxygen, parasites perform anaerobic glycolysis. No production of ATP is described to occur via oxidative phosphorylation as tricarboxylic acid (TCA) cycle, respiratory chain and oxidative phosphorylation machinery are highly repressed[11].

In trypanosome glycolysis, the first seven glycolytic enzymes are sequestered in peroxisome-like organelles called glycosomes, in which glucose is converted into 3-phosphoglycerate. The final reactions, catalysing the conversion of 3-phosphoglycerate into pyruvate occurs in the cytoplasm[12]. Since the glycosomal membrane is impermeable to glycolytic metabolites[13], ATP balance is maintained inside the organelle and no net ATP production takes place: two ATP-consuming reactions in the upper

part are compensated by two ATP-producing reactions in the lower part. Therefore, net ATP production relies solely on the cytoplasmic steps (**Figure 2A**).

In addition to ATP balance, NADH balance is also maintained inside the glycosome. NADH formed by glyceraldehyde 3-phosphate dehydrogenase (**step 8, Figure 2A**) is re-oxidized by the reduction of dihydroxyacetone phosphate (DHAP) to glycerol 3-phosphate (G3P) (**step 6, Figure 2A**). In the presence of oxygen, although multiple mitochondrial functions are repressed in BSF, G3P is converted to DHAP through a short respiratory system that includes a so-called trypanosome alternative oxidase (TAO) present in the mitochondrial membrane. The formed DHAP re-enters the glycosome and feeds the pyruvate branch (**step 5, Figure 2A**). Thus, in the presence of oxygen, 2 molecules of pyruvate are formed, yielding 2 ATP per glucose[11,14] (**Figure 2A**).

Under low oxygen levels, DHAP is converted to G3P and further converted to glycerol plus ATP (**steps 6 and 7, Figure 2A**). Therefore, anaerobic glycolysis presents a net production of 1 ATP per glucose. Although this mechanism allows the parasites to overcome short periods of anaerobiosis, it is insufficient to sustain growth as incubating BSF under anaerobic conditions leads to cell death[15] (**Figure 2A**).

- **Procyclic forms**

Upon uptake of BSF parasites by a tsetse fly, during a blood meal, parasites undergo differentiation to PCF, which is accompanied by considerable changes in energy metabolism. Alike BSF, PCF parasites are also able to catabolise glucose, through glycolysis, being its preferred carbon source[16]. However, PCF possess a fully developed mitochondrion, thus the end-product of glycolysis, pyruvate, is not excreted but further metabolised to acetyl-CoA. Surprisingly, although genes and protein expression for all eight enzymes of the TCA cycle are present, the formed acetyl-CoA is not degraded to CO_2 by the TCA cycle[17]. In PCF, acetyl-CoA is converted into acetate and succynil-CoA by the acetate:succinate CoA-transferase (ASCT). Succynil-CoA is then converted by succynil-CoA synthetase, leading to the production of 1 ATP[18] (**Figure 2B**).

Nevertheless, in the tsetse midgut, glucose is only available briefly after a blood meal. Therefore, PCF rely on the catabolism of aminoacids in the mitochondrion, mainly proline and threonine. Proline is metabolised and excreted from the cell as the end-product alanine[19] while threonine is degraded to acetate which in turn feeds lipid biosynthesis[20]. Both catabolic pathways lead to the production of large amounts of NADH which are re-oxidized by the respiratory chain, also present in PCF, followed by the consequent production of ATP by ATP synthase (**Figure 2B**).

As mentioned previously, the TCA cycle is present in PCF but not functioning as a true cycle. Why this happens is still a matter of speculation. It is conceivable that perhaps the activities of some of the cycle's enzymes are too low compared with, for example, ASCT, that would route all acetyl-CoA towards acetate production[11]. However, clear functions have been attributed to parts of the cycle. For instance, the cycle's conversion of α-ketoglutarate to succinate is used for proline catabolism (**Figure 2B, orange**). It has also been suggested that the part of the formation of citrate is used for fatty acid biosynthesis (**Figure 2B, purple**). Finally, the part of the cycle in which succinate is converted to malate is used for gluconeogenesis, when parasites proliferate in the absence of carbohydrates[21] (**Figure 2B, blue**).

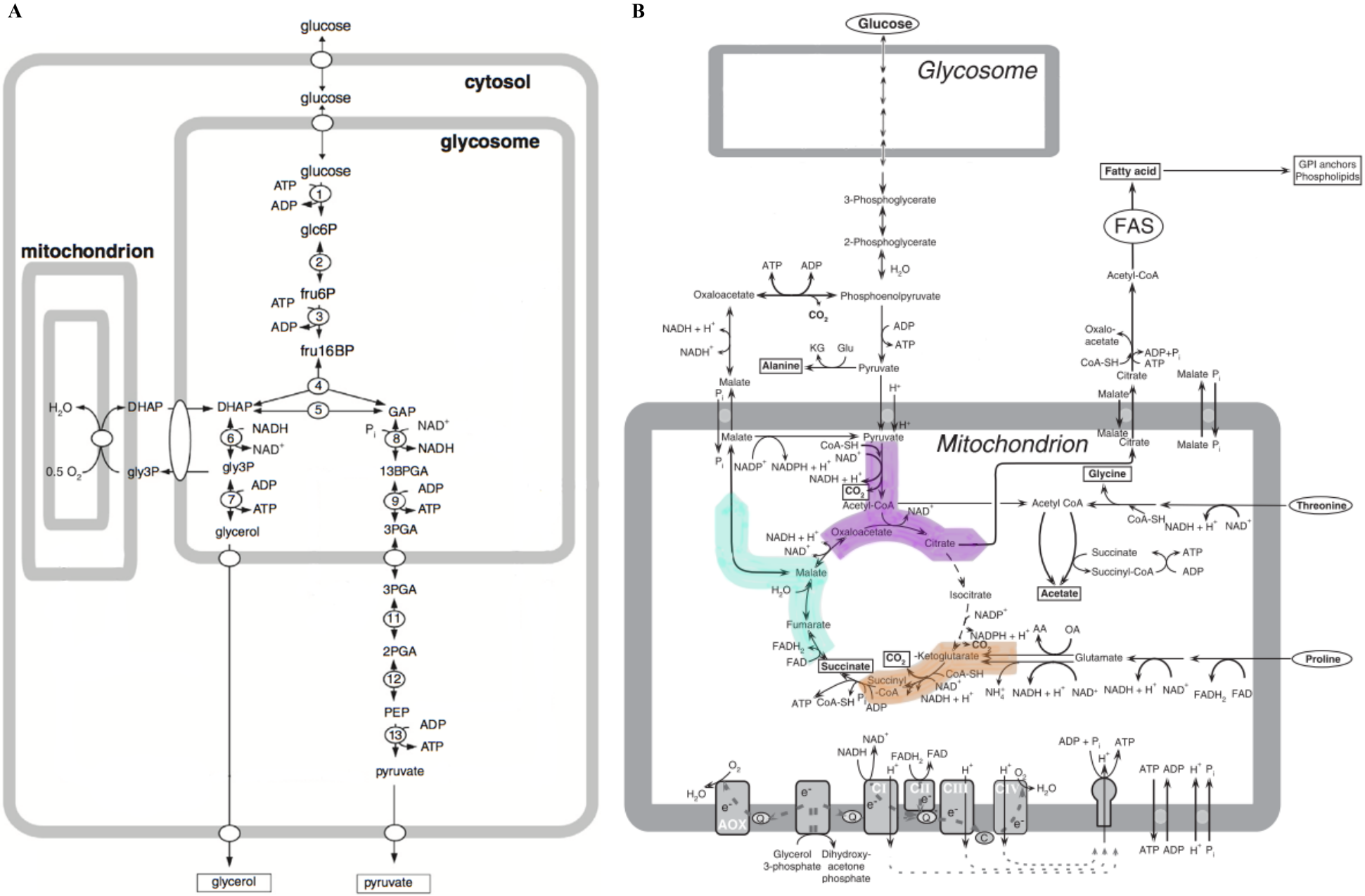

Figure 2. Energy metabolism in. *T. brucei* **(A)** BSF parasites. Adapted from 14. **(B)** PCF parasites. Adapted from 11.

- **Adipose tissue forms**

Energy metabolism of ATF parasites has not been thoroughly studied to date, due to its recent discovery. However, it is conceivable that parasites adapt their metabolism to the novel environment, upon entry in AT. To this regard, it was shown that ATF parasites are able to rewire their gene expression to adapt to the AT environment[9]. The most prominent finding is the possibility of ATF parasites using fatty acid catabolism as an energy source since the putative genes for the second and fourth steps of the β-oxidation pathway were upregulated at the RNA level, when compared with BSF. Additionally, ATF parasites were shown to be able to uptake and catabolise fatty acids through β-oxidation. One possible scenario would be that the formed acetyl-CoA could feed the also seemingly active tricarboxylic acid (TCA) cycle, as three key enzymes are upregulated in ATF parasites. The TCA cycle would produce NADH and $FADH_2$ which would lead in turn to ATP production by oxidative phosphorylation. Alternatively, and alike PCF, acetyl-CoA, the end product of β-oxidation, could be converted into acetate leading to the production of one molecule of ATP. Together, this suggests that interestingly, although derived from BSF, the energy metabolism of ATF parasites also comprises pathways previously detected in PCF.

Overall, β-oxidation is the strongest candidate for an energy metabolism adaptation in ATF parasites. Since AT is a fatty acid-rich environment, it can be argued that performing β-oxidation might constitute a mechanism that increases parasite fitness, thus accumulating and persisting in this organ.

1.4. Immune response against *Trypanosoma* infection

Upon transmission to the mammalian host, trypanosomes elicit an innate immune response and later an adaptive immune response. The latter requires an efficient antigen presentation, activation and development of effector T and B lymphocytes. Below, the contribution of myeloid, B and T cells in the immune response against *Trypanosoma* infection will be addressed. Furthermore, through co-evolution with their hosts, trypanosomes have learnt to cope with the host immune system, evolving mechanisms to hinder an effective immune response[22]. Thus, antigenic variation and other strategies employed by parasites to prevent immune elimination, will also be mentioned.

1.4.1. Myeloid cell function

Cells of the myeloid lineage confer the first line of defence against *T. brucei* infection, being essential for the establishment of innate and adaptive immune responses that protect the host from uncontrolled parasite growth. Macrophages are activated by parasite factors, such as glycosylphosphatidylinositol (GPI) anchor of variant surface proteins (VSGs) and trypanosomal DNA, leading to the production of pro-inflammatory cytokines and antigen presentation to T cells. This type of macrophages is termed M1-type. In later stages, macrophages produce anti-inflammatory cytokines to avoid a sustained inflammatory response and ensure longer survival of the host, being termed M2-type macrophages.

- **Pathogen recognition and macrophage activation**

Pathogen recognition is mediated by the interaction of pathogen-associated molecular patterns (PAMPs) and pattern recognition receptors (PRRs), such as the toll-like receptors (TLRs), present on neutrophils, macrophages and dendritic cells (DCs). Upon activation, neutrophils phagocyte pathogens, secrete granules with antimicrobial proteins or form neutrophil extracellular traps (NETs). In turn,

macrophages and DCs phagocyte pathogens and modulate downstream events that lead to an adaptive immune response[23,24].

In the case of trypanosomiasis, the main trigger of the innate immune response involves the interaction between macrophages and the GPI anchor of variant surface glycoproteins (VSGs), the most abundant protein in *T. brucei*, covering the entire parasite surface. During infection, a membrane-associated phospholipase C (PLC) hydrolyses the GPI anchor of the membrane form of VSG (mVSG), releasing a soluble form VSG (sVSG)[25]. Although the identity of the receptor that recognizes the residual GPI anchor in the membrane or in the sVSG remains elusive, it has been suggested to be part of the TLR family, signalling through myeloid differentiation primary response gene 88 (MyD88)[26]. Furthermore, trypanosomes contain DNA with unmethylated CpG sequences that is released after parasite elimination/lysis, leading to macrophage activation via TLR9 signalling[27]. Neutrophil contribution for the early response against *T. brucei* infection has not been reported to date, however the contribution of these phagocytes is documented in many other protozoan infections[28–30].

MyD88- and TLR9-mediated responses lead to classically activated (also known as M1) macrophages which phagocyte parasites and secrete pro-inflammatory cytokines such as interferon-gamma (IFN-γ), interleukin (IL)-12, tumour necrosis factor alpha (TNF-α)[26,27]. Furthermore, being antigen presenting cells (APCs), macrophages will activate T lymphocytes (addressed in the next section), generating an adaptive immune response. Such inflammatory response is essential to control parasite growth, mainly in the first parasitemia peak which is more aggressive. However, although beneficial for the host in early stages of infection, a sustained inflammation has a pathological outcome. Thus, in later stages, M1 macrophages and their pro-inflammatory cytokines are downregulated, giving rise to alternatively activated (M2) macrophages. M2 macrophages are characterized by the expression of anti-inflammatory cytokines, such as IL-4, IL-10, IL-13, transforming growth factor beta (TGF-β), being involved in tissue healing and avoiding immunopathology (longer survival of the host)[31].

1.4.2. T cell function

T lymphocytes are essential for resistance against trypanosomiasis. In early stages of infection, CD4+ and CD8+ T lymphocytes limit parasite growth through the production of pro-inflammatory cytokines, mainly IFN-γ and TNF-α. Later, regulatory T (Treg) lymphocytes mediate the downregulation of the inflammatory response, possibly through the production of IL-10, protecting the host from tissue damage.

- **Production of IFN-γ**

IFN-γ production is essential for parasite growth control, during *T. brucei* infection. Such importance was depicted in IFN-γ-deficient mice infected with *T. brucei* which present a higher parasitemia peak and shorter survival time[32]. There are two main triggers for IFN-γ production by T lymphocytes. On one hand, sVSG and trypanosomal DNA activate M1 macrophages, which secrete pro-inflammatory cytokines, such as IFN-γ and TNF-α, and perform MHC-II antigen presentation. Both processes lead to the activation of CD4+ and CD8+ T lymphocytes and further production of IFN-γ and TNF-α[26,27]. On the other hand, IFN-γ production is also elicited by a molecule secreted by the parasite, termed trypanosome lymphocyte triggering factor (TLTF), which induces an upregulation of IFN-γ secretion in CD8+ T cells[33]. However, contrary to IFN-γ-deficient mice, in CD8-deficient mice infected with *T. brucei*, parasitemia was lower and mice survived longer, suggesting a beneficial role for the parasite[33]. This is in agreement with studies that have proposed IFN-γ to be a growth stimulus for *T. brucei*, even though the mechanism of action dependent on CD8 T cells remains elusive[33,34].

- **Production of TNF-α**

TNF-α, produced by activated T cells and M1 macrophages, is also involved in growth control of *T. brucei*. The role of TNF-α in reducing parasite burden was first suggested for its ability to lyse parasites isolated during the peak of parasitemia, *in vitro*[35]. It was further corroborated *in vivo*, as parasite development in TNF-$\alpha^{-/-}$ mice infected with *T. brucei* reached an extremely high parasitemia peak[36]. However, parasites have developed the ability to counteract TNF-α action and establish infection. Under stress conditions, parasites upregulate *T. brucei* adenylate cyclase (TbAdC), a transmembrane protein that converts ATP into cyclic adenosine monophosphate (cAMP). Thus, upon phagocytosis, TbAdC is upregulated, cytoplasmic cAMP levels increase within the phagocyte, activating protein kinase A and leading to the inhibition of TNF-α production[37]. Therefore, an altruistic mechanism seems to have formed, whereby phagocytosed parasites inhibit TNF-α trypanocidal action, allowing the other parasites to initiate the first wave of parasitemia.

- **Downregulation of inflammatory response**

As mentioned before, although controlling parasite growth, a sustained pro-inflammatory response is harmful for the host. Hence, in later stages of infection, this response is substituted by an anti-inflammatory one. Treg cells and production of IL-10 have been suggested to be main players in the regulation of this switch. During infection with *T. brucei*, induced expansion of Treg cell population lead to a downregulation of IFN-γ, TNF-α and ROS, delayed the onset of liver injury, reduced anaemia and prolonged survival of infected mice[38]. This indicates that Treg cells are able to supress the type 1 inflammatory response and limit tissue damage. In turn, IL-10 is produced by CD4+ T cells (Treg and non-Treg cells). The absence of this cytokine rendered IL-$10^{-/-}$ mice highly susceptible to infection, resulting in death within one week[32]. This suggests that IL-10 is essential for survival, possibly by restricting extreme inflammatory responses.

Moreover, although not described in a *T. brucei* infection to date, PD-1/PD-L1 pathway is also responsible for the downregulation of the inflammatory response. PD-1 is an immunoinhibitory receptor, also known as immune checkpoint, that negatively regulates T cell activation, following PD-L1 engagement. This limits activated T cell function by generating exhausted/unresponsive effectors, thus preventing autoimmunity and tissue damage[39].

1.4.3. B cell function

B lymphocytes are critically important for the control of *T. brucei* infection through the continuous interplay between the parasite surface, covered by VSGs, and antibodies. B cells produce antibodies that opsonize and lead to the clearance of the parasites. An indicator of the importance of antibodies in the clearance of the parasite lies in one of the main evasion mechanism of *T. brucei*, antigenic variation, whereby the parasite-coating VSG changes and anti-VSG antibodies being produced no longer recognize the parasite. The expression of another VSG gives rise to a new population of proliferating parasites until a specific immune response is again mounted. Therefore, this host-parasite interaction is responsible for the characteristic waves of parasitemia displayed throughout the disease and highlights the key role played by B cell response in controlling infection.

- **Polyclonal B cell activation**

Early stages of *T. brucei* infection are characterized by a polyclonal B-cell activation. This is present in both murine and bovine trypanosomiasis, evidenced by significant high levels of plasma immunoglobulins, upon infection[40,41]. It has been suggested that parasite factors, such as trypanosomal DNA and VSG, trigger this natural innate immune response, which leads to production of antibodies to cope with parasite proliferation, thus containing pathogen dissemination[42,43].

However, induction of polyclonal B cell response might also be regarded as an immune evasion mechanism. By unselectively differentiating B cells into plasma cells (antibody-producing cells), a significant component of such antibodies is either polyspecific or autoreactive[41,44,45], diluting the specific response against parasite antigens.

- **Specific anti-VSG B cell response**

B-cells are crucial in parasite clearance and control of infection, as evidenced in B cell-deficient mice that fail to clear parasites and have a shorter survival time, following *T. brucei* infection[46]. This protection conferred by B cells is obtained through the production of specific antibodies that opsonize parasites, leading to sensitivity to complement activity and phagocytosis by macrophages. Since the surface of *T. brucei* parasites is entirely coated by VSG, these specific antibodies are raised mainly against epitopes of such protein, through T cell-dependent and T cell-independent pathways[47]. Of note, mice immunized with VSG or irradiated trypanosomes are protected against a challenge with homologous parasites, highlighting the role of VSG in inducing an immune response and immunologic memory[48].

During the first days of *T. brucei* infection, B cells generate a rapid IgM response, which is followed by an immunoglobulin isotype switch and secretion of high levels of IgG2a, IgG2b and IgG3 antibodies[49]. Thus, anti-VSG IgMs are the first line of antibodies to be produced, being extremely important for the clearance of the first parasitemia peak. In fact, the presence of anti-VSG IgGs was only detectable after the first peak[50]. More recently, it was shown in infected IgM-deficient mice that, even though mortality was slightly increased, parasitemia was controlled almost as well as in wild-type mice[46]. At first, this could reveal a minor role of IgMs in controlling parasitemia, contrarily to what was reported before. However, an increase of IgDs was also observed in infected IgM-deficient mice which could constitute a compensation mechanism that clears the parasites, in the absence of IgMs[46]. Taken together, this suggests that B cell response is robust against *T. brucei* and the different immunoglobulin isotypes work together to control infection.

To evade an effective antibody-mediated clearance, *T. brucei* performs antigenic variation, which will be discussed below. Furthermore, an additional aspect that reduces antibody-mediated clearance efficiency is that, although specific antibodies are raised against different parts of the VSG molecule[51], only surface exposed epitopes (N-terminal and variable region) can play a role in parasite elimination, whereas buried regions (C-terminal and conserved region) are inaccessible to conventional antibodies[52].

- **Antigenic variation**

Antigenic variation is the main immune evasion mechanism used by *T. brucei* to ensure a successful infection in the mammalian host. To this end, BSF are entirely covered by a densely-packed array of 10 million identical copies of VSG proteins[53], which, as mentioned previously, are the prime target for antibody response. This coat is periodically changed to a different VSG type, independently of antibody response[46], by manipulating VSG gene expression[53]. Therefore, following infection and during the ascending phase of parasitemia, the majority of parasites express the same VSG. The host's immune

system recognizes the VSG and produces antibodies against it. As the parasites that express this VSG are eliminated, along with the differentiation of slender forms into non-dividing stumpy forms[54], parasitemia enters a descending phase. At the same time, parasites that had already changed the type of expressed VSG are not recognized by antibodies and proliferate, giving rise to a new wave of parasitemia and a long-lasting chronic infection[55] (**Figure 3**).

Of note, in an experimental infection, due to the formation of heterogeneous populations with different types of expressed VSG, along with the unspecific polyclonal B cell response, the mounted immune response is slightly different in each infected mouse. Consequently, parasitemia curves share common trends, especially in the early stages of infection, but are subject to individual variability (**Figure 3**).

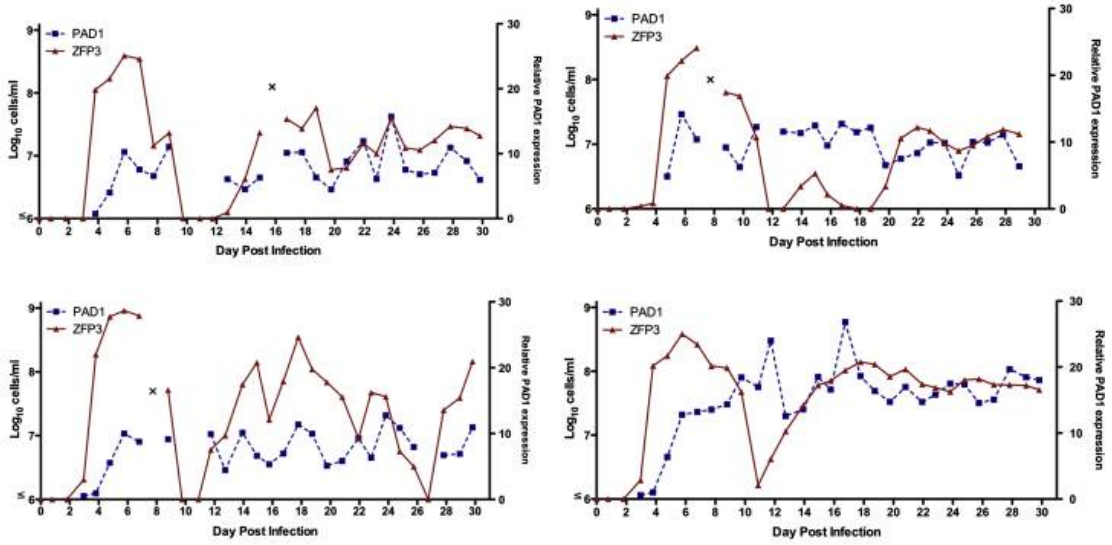

Figure 3. Dynamics of infection with *T. brucei* in mice. (A-D) Different mice infected with *T. brucei* **(Red, Left-hand axis)** Parasite numbers determined by qRT-PCR of constitutive TbZFP3 gene. **(Blue, Right-hand axis)** Stumpy form proportion determined by stumpy-specific PAD1 marker expression. Adapted from 54.

1.5. Adipose tissue immune cell subsets

AT is no longer only considered to play a role in energy and lipid storage and protection against heat loss. Instead, it has been accepted as an endocrine organ[56], as adipocytes secrete a wide variety of hormones and proteins, as well as an immunologically active organ[57]. In lean animals, an anti-inflammatory environment is maintained by resident immune cells, such as macrophages, regulatory T cells and IL-17-producing γδ T cells.

Certain protozoan parasites infect AT and challenge this anti-inflammatory balance. For instance, *Neospora caninum*, the causative agent of neosporosis, is an intracellular protozoan parasite that infects a wide range of nucleated cells, including adipocytes[58]. Upon infection, *N. caninum* elicits a shift towards a pro-inflammatory environment in AT.

1.5.1. Macrophages

Macrophages are the most abundant resident immune cells in AT, in the lean state, constituting up to 75% of all immune cells in this organ[59]. These have been implicated in a myriad of functions that ensure AT homeostasis. M2-like macrophages in AT contribute for maintenance of the anti-inflammatory milieu through IL-4 and IL-10 secretion[60]. In addition, these AT-associated macrophages participate in angiogenesis, proliferation and differentiation of adipocyte precursors and remodelling of extracellular matrix[61,62]. Furthermore, macrophages store iron to avoid iron toxicity in adipocytes[63] and, during cold exposure, produce catecholamines to induce beiging of white AT, which generates heat[64]. One of the particularities of these AT macrophages is that they are self-maintaining tissue-resident subsets. Moreover, the homeostasis and functionality of these macrophages has been linked to peroxisome proliferator activated receptor gamma (PPARγ)[65], also required for adipocyte differentiation[66].

Upon *N. caninum* infection, monocyte-derived macrophages are recruited to AT and the anti-inflammatory environment is skewed towards a pro-inflammatory one. Consequently, M1-like macrophages accumulate and produce IFN-γ to establish a Th1 response, promoting pathogen elimination[58].

Interestingly, lipolysis has also been shown to promote macrophage recruitment to AT in order to remove excess free fatty acids, in lean mice[67].

1.5.2. Regulatory T cells

Treg cells, defined by the expression of Foxp3, are also highly enriched in AT, comprising up to 15% and 40-70% of CD4+ T cells in gonadal AT of 10-weeks and 20-weeks old mice, respectively. These cells are suppressive and promote AT homeostasis by limiting inflammation through IL-10 production[68]. Importantly, AT resident Treg cells are distinct from their circulating counterparts in lymphoid organs based on their transcriptional profile, T cell receptor repertoire, and cytokine and chemokine receptor expression pattern. In addition, and similarly to AT-resident macrophages, PPARγ was found to be a critical molecular orchestrator of Treg cell accumulation, phenotype and function in AT.

In a *N. caninum* infection, following establishment of a Th1 response in AT, Treg cell numbers increase to prevent an excessive inflammatory response. Nevertheless, Th1/Treg ratio is higher in infected animals, when compared with controls, which explains the effectiveness in parasite elimination[58].

1.5.3. IL-17-producing γδ T cells

γδ T cells are segregated according to the cytokine they produce. Two main subsets have emerged as IFN-γ- and IL-17-producing effectors. Recently, AT was identified as a tissue with preferential accumulation of IL-17-producing γδ T cells[69]. Unexpectedly, these IL-17-producing γδ T cells were found to contribute to AT homeostasis through the *in situ* regulation of Treg cells. Kohlgruber *et al.*[69] proposed a novel mechanism in AT whereby γδ T cells crosstalk with IL-33-producing adipose stromal cells and regulate Treg cell homeostasis. In both IL-17- and γδ T cell-deficient mice, decreased levels of IL-33 were observed, leading to decreased Treg cell numbers.

2. AIMS

AT was recently discovered to be a main reservoir of *T. brucei* in an experimental mouse infection model. Thus, understanding why *T. brucei* persists in AT is a major stepping stone in elucidating infection dynamics. We adopted a dual perspective to address *T. brucei* persistence in AT: a parasite- and a host-oriented perspective. In the parasite-oriented perspective, we hypothesized that parasites accumulate in AT as they adapt their energy metabolism to use the lipids stored in the adipocytes. In the host-oriented perspective, we hypothesized that parasites accumulate in AT as the host immune system is potentially more permissive.

The main aim of this thesis is to dissect if the persistence of *T. brucei* in AT depends on:

1. A potential adaptation of energy metabolism of *T. brucei* parasites
2. A permissive/attenuated local immune response by the host

3. MATERIALS AND METHODS

3.1. Animals

In vivo experiments were performed with male C57BL/6J mice, from Charles River Laboratories International, unless otherwise stated. RAG2-deficient ($RAG2^{-/-}$) and AID-deficient ($AID^{-/-}$), generated on a C57BL/6J background, were obtained from Instituto Gulbenkian de Ciência (IGC). IFN-γ-deficient ($IFN\text{-}\gamma^{-/-}$), γδ T cell-deficient ($TCR\delta^{-/-}$) and IL-17-deficient ($IL\text{-}17^{-/-}$) mice, generated on a C57BL/6J background, were kindly provided by Bruno Silva-Santos laboratory from Instituto de Medicina Molecular (iMM). All experimental mice were 6-10 weeks old. Mice were housed in a Specific-Pathogen-Free barrier facility, at iMM, under standard laboratory conditions: 21 to 22°C ambient temperature and a 12h light/12h dark cycle. Chow and water were available *ad libitum*. All the experimental work involving animals was performed according to the EU regulations and was approved by the Animal Care and Ethical Committee of iMM (AWB_2016_07_LF_Tropism).

3.2. Parasite lines

Experiments were mainly performed using parasites derived from *T. brucei* AnTat 1.1E, a pleomorphic clone derived from the EATRO1125 strain. AnTat1.1E 90-13 is a transgenic cell-line encoding the tetracyclin repressor and T7 RNA polymerase[70]. AnTat1.1E 90-13 GFP::$PAD1_{utr}$ derives from AnTat1.1E 90-13 in which the green fluorescent protein (GFP) is coupled to PAD1 3'UTR. We also used *T. brucei* Lister 427, a monomorphic strain derived from antigenic type MiTat 1.2, clone 221a[71]. In the same way, Lister 427 90-13 is a transgenic cell-line encoding the tetracyclin repressor and T7 RNA polymerase.

To analyse the potential of an energy metabolism adaptation in parasite persistence in AT, the following parasite lines were used: A) *T. brucei* AnTat1.1E 90-13 Δ*tfeα*1/Δ*tfeα*1 which was generated using constructs[72] kindly provided by Dr. Frédéric Bringaud (Université de Bordeaux, Bordeaux, France). B) *T. brucei* Lister 427 90-13 Δ*asct*/Δ*asct*[18] also kindly provided by Dr. Frédéric Bringaud and C) *T. brucei* AnTat1.1E Δ*nubm*/Δ*nubm* and *T. brucei* AnTat1.1E Δ*nukm*/Δ*nukm* kindly provided by Dr. Achim Schnaufer (University of Edinburgh, Edinburgh, United Kingdom).

The local immune response in AT and the effect of IFN-γ on parasite growth, *in vitro*, were studied using AnTat1.1E 90-13 GFP::$PAD1_{utr}$.

3.3. Generation of TFEα-deficient *T. brucei*

TFEα-deficient *T. brucei* (Tb927.2.4130, TriTrypDB) were generated by replacing the first and second *TFEα1* alleles with puromycin (*PAC*) and blasticidin (*BSD*) resistance markers, respectively, in *T. brucei* AnTat1.1E 90-13. Replacement was performed via homologous recombination by transfecting *T. brucei* with DNA fragments containing a resistance marker gene flanked by the *TFEα1* UTR sequences, provided by Dr. Frédéric Bringaud[72] (**Supplementary table 1**).

T. brucei was cultured at 37°C in 5% CO_2 in HMI-11 medium (HMI-9 medium[73] without serum plus) and parasite density was maintained below $5x10^5$ cells/mL. For the transfection, $50x10^6$ cells were harvested by centrifugation (2000 rpm, 10 minutes, 4°C). The cell pellet was resuspended in 100 µL of Tb-BSF buffer (90 mM sodium phosphate, 5 mM potassium chloride, 0.15 mM calcium chloride, 50 mM HEPES, pH7.3)[74] with 5 µg of the above DNA fragment, transferred to a cuvette and transfected

with Amaxa Nucleofector II system using the X-001 program. After transfection, cells were immediately transferred to 30 mL of pre-warmed HMI-11 medium. Parasites were plated in 24-well plates using 1/1, 1/10 and 1/100 dilutions. After 7-hour incubation, selective drug was added to culture medium. Approximately 6-8 days post-transfection, resistant clones became detectable, were transferred to fresh selective medium and kept under $5x10^5$ cells/mL.

Confirmation of *TFEα1* allele replacement for the resistance marker was performed by PCR, using a combination of pairs of primers that anneal inside the *TFEα1* coding region, resistance marker coding region and outside the targeting region (**Supplementary table 2**). PCR product was resolved in a 1.2% (m/v) agarose gel pre-stained with GelRed (Biotium).

To make cryostabilates of TFEα-deficient *T. brucei*, $1.5x10^6$ parasites were harvested by centrifugation (2000 rpm, 10minutes, 4°C) and resuspended in 500µL of HMI-11 with 10% (v/v) glycerol. Cryostabilates were kept at -80°C.

3.1. Determination of *T. brucei* growth rate in the presence of murine IFN-γ

To test if IFN-γ has an effect on parasite growth *in vitro*, *T. brucei* was cultured in HMI-11 supplemented with murine IFN-γ (Peprotech, 315-05), at the final concentrations of 0.1, 1, 10 and 100 ng/mL. As a control, *T. brucei* was also cultured in HMI-11 without IFN-γ.

To calculate growth rate in each condition, cell densities were determined every 24 hours and cumulative growth curves were plotted taking into account the dilution factors necessary to maintain cultures below a density of 5×10^5 cells/mL. Growth rate corresponds to θ in the equation $y = \gamma e^{\theta t}$ obtained by exponential regression. Doubling time (DT) is given by $DT = \frac{\ln(2)}{\theta}$. Fold increase per day (24 hours) is given by $fold\ increase = 2^{\frac{24}{DT}}$.

3.2. Mice experimentation

Prior to infection, *T. brucei* cryostabilates were thawed and parasite mobility was checked under an optic microscope. Mice were infected by intraperitoneal (i.p.) injection of 2000 *T. brucei* parasites. At selected time-points post-infection, animals were euthanized by CO_2 narcosis and immediately perfused transcardially with pre-warmed heparinised saline (50mL phosphate buffered saline (PBS) with 250 µL of 5000 I.U./mL heparin). Organs were collected and either snap frozen in liquid nitrogen or used immediately to prepare single cell suspensions for flow cytometry staining.

To block PD-1/PD-L1 axis, mice were inoculated with 300µg of αPD-1 (clone RMP1-14, InVivoMab, BioXcell), intravenously (i.v.), before infection and at days 3, 5 and 7 post-infection.

3.3. Parasite quantification in blood and organs

For parasitemia quantification, blood samples were taken daily from the tail vein and parasite counts were performed manually in a haemocytometer (detection limit is 10^6 parasites per mL of blood). When applicable, total parasite number was determined by multiplying by the total volume of blood, calculated considering that a mouse has 58.5 mL of blood per kg of bodyweight[75].

For parasite quantification in organs, genomic DNA (gDNA) was extracted using NZY tissue gDNA isolation kit (NZYTech, Portugal). By qPCR, the amount of *T. brucei* 18S rDNA present in the tested organ was measured and converted into numbers of parasites using a calibration curve[9]. Parasite numbers per mg of organ (parasite density) were then calculated by dividing parasite numbers for the

weight of organ used for qPCR. The total amount of parasites in the organ was estimated by multiplying parasite density by the total weight of the organ.

3.4. Preparation of single cell suspensions

Gonadal AT samples were incubated at 37°C in Dulbecco's Modified Eagle Medium (DMEM, GIBCO) with Collagenase I (0.4mg/mL, Whortington LS004196), Collagenase IV (1mg/mL, Whortington LS004188) and DNAse (10µg/mL) for 30 minutes, under 1100 rpm agitation. Single cell suspensions from the spleen and digested gonadal AT were obtained by sieving them through a 40-µm-pore-size nylon cell strainer (BD Biosciences) with a syringe plunger. Spleen cells were treated with erythrocyte lysis buffer (BioLegend 420301) to lyse red blood cells. Both spleen and gonadal AT cells were resuspended in complete Roswell Park Memorial Institute medium (cRPMI, RPMI supplemented with 1% sodium pyruvate 100mM, 1% MEM non-essential amino acids, 1% HEPES 1M, 1% Pen-Strep, 0.1% gentamycin 50mg/mL, 0.1% β-mercaptoethanol 50mM and 10% fetal calf serum (all from Gibco)) to use for flow cytometry analysis. Live cells in single cell suspensions were counted after trypan blue staining in a haemocytometer.

3.5. Flow cytometry

Stainings of myeloid and lymphoid cells were performed separately. In isolated spleen cells, staining was performed in $5x10^6$ cells. In isolated gonadal AT cells, due to lower isolation yield, staining was performed in the higher number of cells possible, by using half of cell suspension in each staining.

For myeloid staining of surface antigens, cells were incubated for 45 minutes at 25°C in cRPMI, in the presence of 5% normal mouse serum (NMS), with the following antibodies: F4/80-FITC (clone BM8, BioLegend), Ly6G-PerCP/Cy5.5 (clone 1A8, BioLegend), CD274-PE/Cy7 (PD-L1, clone 10F.9G2, BioLegend), CD11b-APC/Cy7 (clone M1/70, BioLegend), CD45-Brilliant Violet (BV) 510 (clone 30-F11, BioLegend) and Ly-6C-BV605 (clone HKL4, BioLegend). To stain non-viable cells, Zombie Violet Fixable Viability Kit (BioLegend) was used, incubating cells in PBS with 5% NMS, for 15 minutes at 25°C. Finally, stained cells were resuspended in cRPMI for flow cytometry acquisition.

For lymphoid staining, cells were first incubated in cRPMI with phorbol 12-myristate 13-acetate (20ng/mL, PMA) and ionomycin (1µg/mL) to stimulate cytokine production by T cells, for 1h45 at 37°C. Next, to block cytokine endocytosis, cells were incubated in cRPMI with brefeldin A (10µg/mL) and monensin (5µM), for 1h at 37°C. Staining of surface antigens was performed by incubating cells for 45 minutes at 25°C in cRPMI with 5% NMS and the following antibodies: CD3-FITC (clone 17A2, BioLegend), CD279-PE (PD-1, clone J43, eBioscience), CD45-BV510 (clone 30-F11, BioLegend) CD4-BV605 (clone RM4-5, BioLegend) and CD8-BV711 (clone 53-6.7, BioLegend). To stain non-viable cells, LIVE/DEAD Fixable Near-IR Dead Cell Stain Kit (Invitrogen) was used, incubating cells in PBS with 5% NMS, for 15 minutes at 4°C. For staining of intracellular antigens, fixation and permeabilisation of cells was performed using Foxp3/Transcription Factor Staining Buffer Set (eBioscience) and the following antibodies: IFN-γ-PerCP/Cy5.5 (clone XMG1.2, BioLegend), Foxp3-APC (clone FJK-16s, BioLegend) and TFE-α-eFluor450 (clone MP6-XT22, BioLegend). Finally, stained cells were resuspended in cRPMI for flow cytometry acquisition.

Samples were acquired on a BD LSRFortessa flow cytometer with FACSDiva 6.2 Software. All data were analysed using FlowJo X version 10.0.7r2 software. A schematic of the gating strategy used is represented below (**Figure 4**).

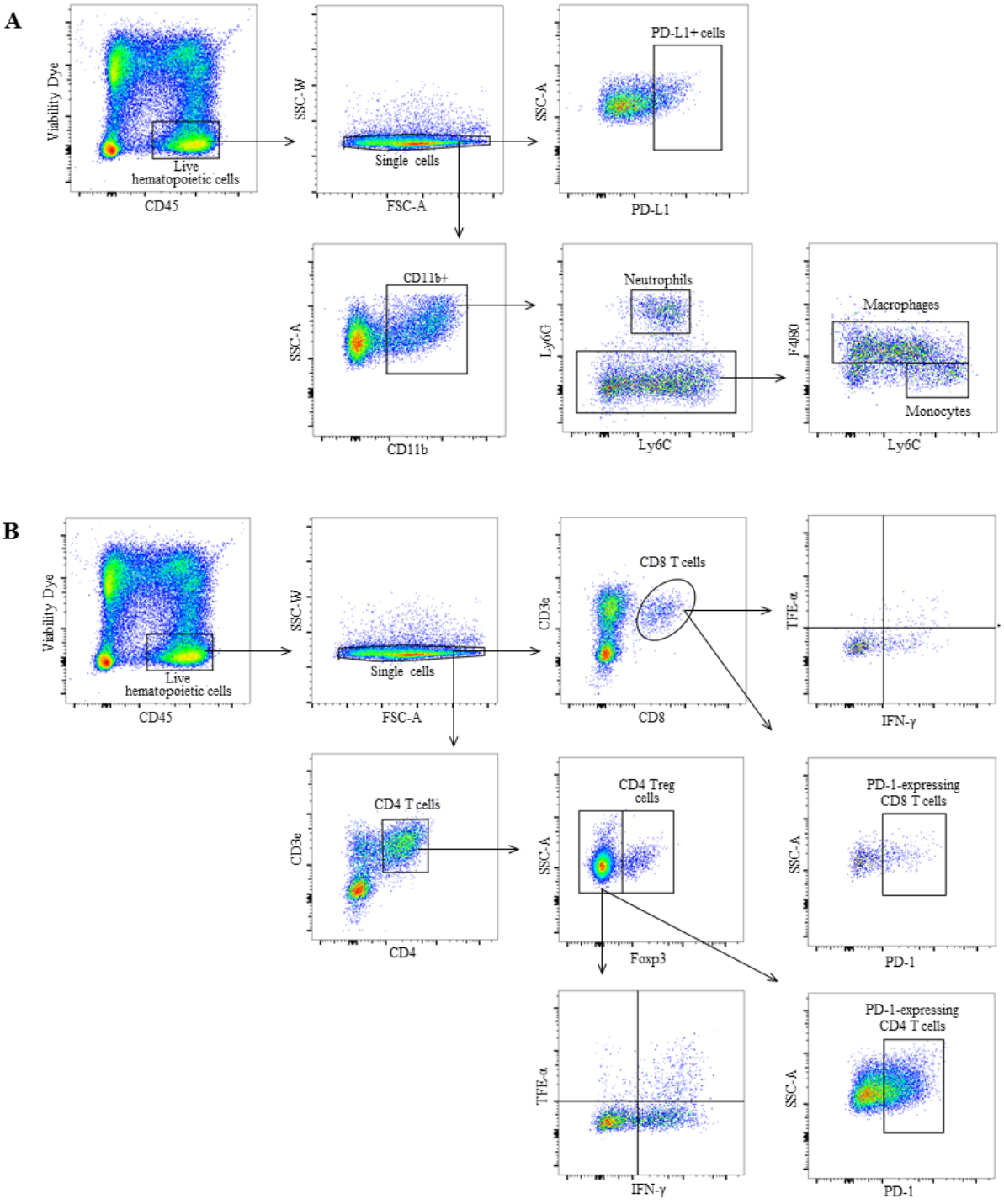

Figure 4. Gating strategy for flow cytometry analysis. **(A)** Myeloid cells. **(B)** Lymphoid cells.

4. RESULTS

4.1. Energy metabolism in *T. brucei* persistence in adipose tissue

In this project, we hypothesized that *T. brucei* parasites occupying AT are able to use fatty acids stored in the adipocytes and catabolise them via β-oxidation. In one scenario, acetyl-CoA, the end product of β-oxidation, would feed the TCA cycle, generating NADH and $FADH_2$, which would lead in turn to ATP production by oxidative phosphorylation. In an alternative scenario, the acetyl-CoA could be converted into acetate, leading to the production of ATP via substrate phosphorylation, while shorter fatty acids may be used as building blocks to synthesize other more complex lipids. To investigate whether parasites have increased fitness in AT due to catabolism of fatty acids, through the above-mentioned pathways, mice were infected with *T. brucei* parasites deficient in three key enzymes of such pathways (**Figure 5**).

- β-oxidation was impaired by knocking-out a putative gene responsible for the second step of β-oxidation, TFEα (Tb927.2.4130, TriTrypDB)[72]. The knock-out was done using knock-out constructs kindly provided by our collaborator Dr. Frédéric Bringaud, in a pleomorphic background, ensuring the presence of both slender and stumpy forms in mice infections.
- To block conversion of acetyl-CoA to acetate, and subsequent production of ATP, we used ASCT-deficient *T. brucei* (Tb927.11.2690, TriTrypDB) (also provided by Dr. Frédéric Bringaud), in a monomorphic background. Since this knock-out was done in a monomorphic background, slender forms do not differentiate to stumpy forms, conferring higher virulence. Unpublished data from our laboratory showed that ASCT was upregulated at the protein level in ATF parasites.
- To block oxidative phosphorylation, null mutants for NUBM (Tb927.5.450, TriTrypDB) and NUKM (Tb927.11.1320, TriTrypDB) were kindly provided by our collaborator Dr. Achim Schnaufer, in a pleomorphic background. NUBM and NUKM are core proteins from the respiratory chain's complex I (NADH:ubiquinone oxidoreductase), suggesting that either null mutant should render the complex I and respiratory chain inactive.

If these genes/pathways are necessary for accumulation of *T. brucei* in AT, then in a mouse infected with a null mutant we would expect the gonadal AT to have a diminished parasite burden.

Organs from mice infected with TFEα$^{-/-}$ were collected at 6 and 13 days post-infection (dpi), which comprise the peak of parasitemia and a time-point right after parasite growth recovery. Organs from mice infected with ASCT$^{-/-}$ were collected at 5 dpi, since, due to the lack of differentiation to stumpy forms, mice rapidly succumb to hyperparasitemia. Organs from mice infected with NUBM$^{-/-}$ and NUKM$^{-/-}$ were also collected at 5 dpi as, although generated in a pleomorphic strain, lack of slender to stumpy differentiation had been described by our collaborator Achim Schnaufer. Parasitemia was quantified by counting *T. brucei* numbers in a haemocytometer. *T. brucei* total numbers in heart, gonadal AT, kidney and liver were quantified by qPCR, as previously published[9].

Both TFEα$^{-/-}$ and ASCT$^{-/-}$ infections displayed a pattern of parasitemia similar to wt (**Figure 5A, middle and Figure 5B, middle**). For TFEα$^{-/-}$, no significant change was observed in parasite numbers in the gonadal AT and heart, suggesting that this gene is not essential for parasite accumulation in AT neither at early (6 dpi) and later (13 dpi) time-points (**Figure 5A, bottom**). In the same way, the absence of ASCT did not lead to a decrease in parasite number in gonadal AT, suggesting that production of ATP through the acetate pathway is not responsible for higher parasite fitness in AT (**Figure 5B, bottom**).

Infections with NUBM$^{-/-}$ and NUKM$^{-/-}$ showed hyperparasitemia when compared with the parental cell line. In addition, it was observed, in another experiment (not shown), that at 6 dpi, one day after the studied time-point, parasitemia continued to increase with NUBM$^{-/-}$ and that mice die of hyperparasitemia with NUKM$^{-/-}$ (**Figure 5C, middle**). At 5 dpi, in NUBM$^{-/-}$ infected mice, no impaired accumulation of parasites was observed in gonadal AT. Instead, an even more striking accumulation took place, reaching 10^7 parasites in the organ, which represents a 24-fold difference above the parental cell line (**Figure 5C, bottom**). All other organs also showed an increased parasite load.

The most promising observation was that the absence of NUKM lead to a reduction in parasite load in gonadal AT, representing a 4-fold difference below the less virulent parental cell line, while parasite load was increased in heart, kidney and liver. These results strongly suggest that NUKM is necessary for parasite fitness in AT, but not in blood or other extravascular tissues (**Figure 5C, bottom**).

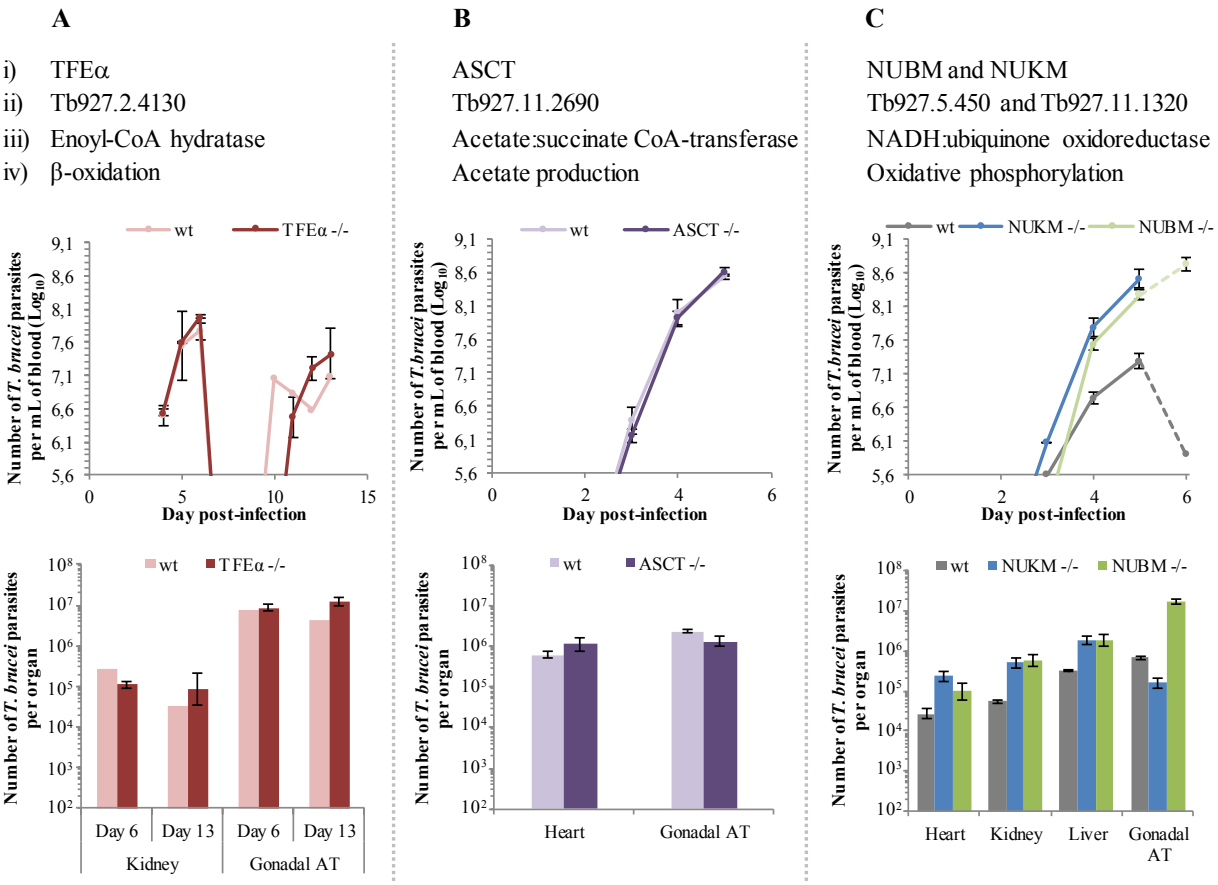

Figure 5. Consequences of parasite metabolic defects in the numbers of vascular and extravascular parasites. (A) Infection of mice with TFEα-deficient *T. brucei* (dark red) or *wt T. brucei* parental line (light red). **(B)** Infection of mice with ASCT-deficient *T. brucei* (dark purple) or *wt T. brucei* parental line (light purple). **(C)** Infection of mice with NUKM-deficient *T. brucei* (blue), NUBM-deficient *T. brucei* (green) or *wt T. brucei* parental line (grey). **(Top)** Information summary of each tested enzyme-deficient *T. brucei*. i) Gene; ii) Gene ID in TriTrypDB; iii) Function; iv) Pathway. **(Middle)** Parasitemia curves of mice infected with *T. brucei* (detection limit is 10^6 parasites per mL of blood). In (C), dashed lines represent the tendency of parasitemia progression between 5 and 6 days after infection. **(Bottom)** *T. brucei* numbers quantified by qPCR in (A) kidney and gonadal AT, 6 and 13 days after infection (B) heart and gonadal AT, 5 days after infection (C) heart, kidney and liver and gonadal AT, 5 days after infection. **(A-C)** Error bars represent the standard error of the mean. (n=2-3 mice per group).

4.2. Dynamics of immune cell populations during *T. brucei* infection

In this project, we hypothesized that *T. brucei* accumulates in AT because this organ may be an immune privileged site favourable for the parasite. AT would become a safe refuge and a reservoir for *T. brucei* to repopulate the blood. However, no characterization of the immune response in AT upon *T. brucei* infection has been reported to date. Consequently, to test this hypothesis, we firstly characterized the immune cell populations in spleen and AT, at key time-points of a mouse *T. brucei* infection. The spleen, a secondary lymphoid organ, was used as a proxy for the systemic immune response, as it filters the blood and is a major site for lymphocyte activation[76]. Additionally, this organ was selected as it provides a higher yield of immune cells than the blood. The analysed time-points were as follows: 4, 5, 6 and 7 days post-infection (dpi), which corresponds to the first peak of parasitemia; 9 dpi, when the host is able to clear the parasite into an undetectable parasitemia; 14, 15 and 16 dpi, when parasite growth recovers and parasitemia is detectable again; lastly, 20, 21, 26, 27 and 28 dpi were tested to account for the small oscillations of parasitemia and parasite burden that occur during the chronic stage of infection.

Parasitemia was quantified by counting *T. brucei* numbers in a haemocytometer. *T. brucei* total numbers in spleen and gonadal AT were quantified by qPCR. Contrary to blood, parasite quantification in the spleen and gonadal AT was only performed for the time-points referred above as it is a terminal process. In the blood, the progression of parasitemia throughout infection exhibited the expected pattern: peak at 5 dpi; undetectable parasitemia between 9 and 13 dpi; followed by fluctuating parasite number that differs between in each mouse (**Figure 6A and B**). In the spleen, the number of parasites reached the peak at 5 dpi and the lowest value at 9 dpi, after clearance (32-fold decrease from 6 to 9 dpi). From 14 dpi, the number of parasites fluctuated at around 10^5 parasites per organ (**Figure 6C**). Finally, the number of parasites peaked at 6 dpi in the gonadal AT, which is one day later than in blood/spleen. From 6 to 9 dpi, parasites underwent clearance, as in blood and spleen, but decreased only 6-fold. From 14 dpi, number of parasites fluctuated at around 10^6 parasites which is approximately 10-fold more than in the spleen (**Figure 6C**).

Immune cell populations were characterized by flow cytometry. We aimed to determine whether the immune response was less active or showed signs of suppression in the AT compared to the spleen. Thus, we focused our analysis on myeloid and T cell subsets. From myeloid cells, known to be important in the innate immune response, we studied the dynamics of macrophages, monocytes and neutrophils. Within T cells, we analysed the production of the two pro-inflammatory cytokines, IFN-γ and TNF-α that participate in the control of *T. brucei* infection. In addition, we compared the frequency of Treg cells in the spleen and AT, which are key promoters of anti-inflammatory response. Finally, we analysed, in T lymphocytes, the expression of PD-1, the inhibitory receptor associated to exhausted/unresponsive effectors. Graphs in the main text showing progression of immune cells per mg of tissue have their equivalent in total cells per organ in the annexes (**Supplementary figure 1 to 6**).

Overall, a gradual but striking infiltration of CD45+ hematopoietic cells was observed in gonadal AT with approximately 5000-fold increase in the number of hematopoietic cells per mg of tissue from 0 to 28 dpi (**Figure 6E**). Although the number of parasites in AT is maximal on 6 dpi, our observations indicate that immune cells are recruited and/or proliferate in AT in a different dynamics, increasing steadily as infection progresses.

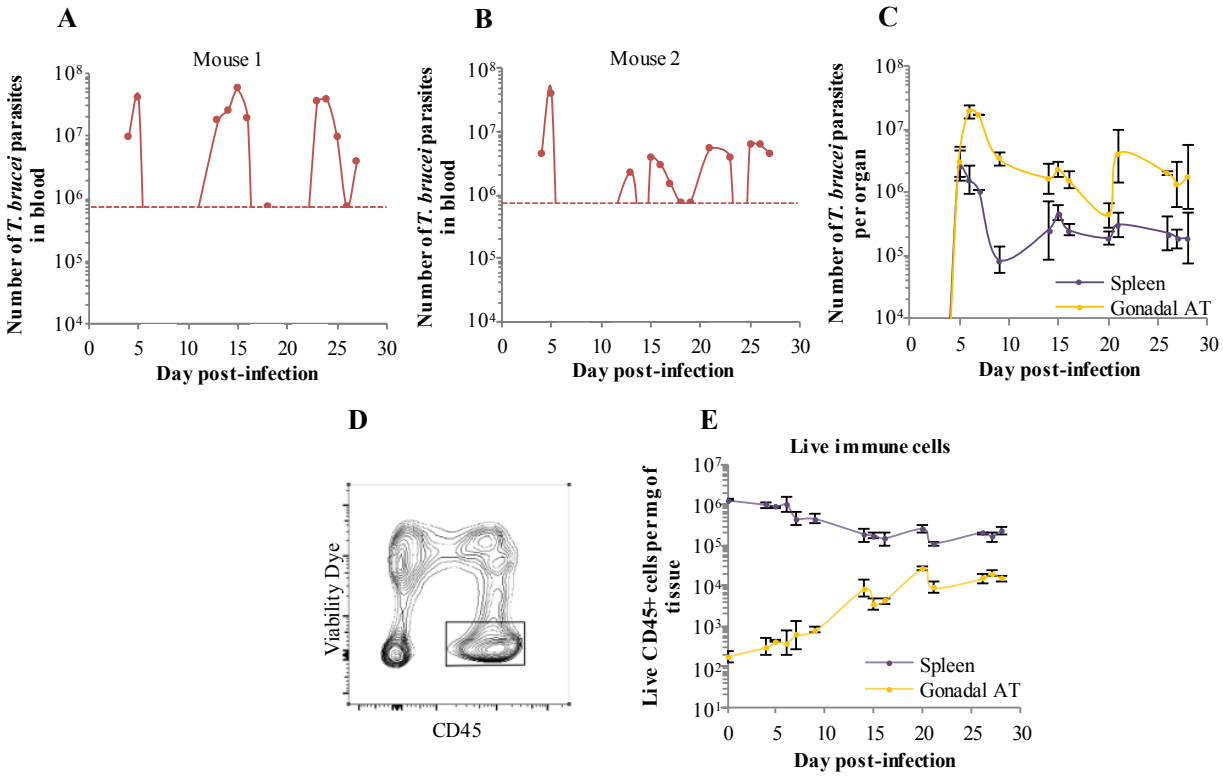

Figure 6. Dynamics of *T. brucei* parasites and immune cells throughout infection. **(A-B)** Total *T. brucei* parasite numbers in blood of infected mice. Comparison highlights variability between different infected mice. *T. brucei* numbers in blood quantified by counting in haemocytometer. Dashed line represents the limit of detection. **(C)** Progression of *T. brucei* numbers in gonadal AT and spleen. *T. brucei* numbers in spleen and gonadal AT quantified by qPCR. **(D)** Contour plot for viability dye/CD45, representing gating strategy for live immune cells (CD45 is a marker for hematopoietic cells). **(E)** Number of live immune cell per mg of tissue in spleen and gonadal AT. **(C,E)** Error bars represent the standard error of the mean (n=2-6 mice per group).

4.2.1. Myeloid cell subsets

To understand if myeloid cells were recruited to AT, upon *T. brucei* infection, we assessed the dynamics of neutrophils (CD11b+Ly6G+), macrophages (CD11b+F4/80+Ly6G-) and monocytes (CD11b+Ly6C+F4/80-Ly6G-) (see gating strategies in **Figure 7A**). We observed that, from 0 to 28 dpi, neutrophils increased 11-fold in the spleen, from 10^3 to 10^4 cells per mg of tissue, and although nearly absent in gonadal AT prior to infection, at 28 dpi reached 10^3 cells per mg of tissue (**Figure 7B**). Macrophages and monocytes oscillated slightly in the spleen around 10^3 cells per mg of organ. In contrast, in the gonadal AT, the number of macrophages and monocytes increased 51-fold to reach approximately 10^3 cells per mg of tissue (**Figure 7C**).

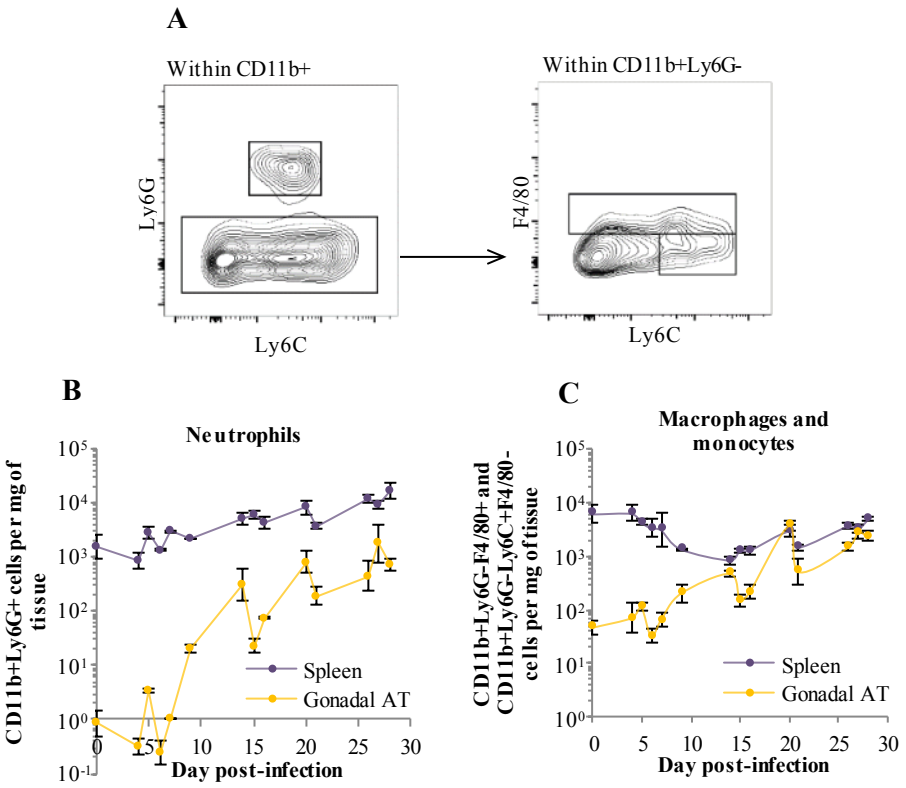

Figure 7. Dynamics of neutrophils, macrophages and monocytes throughout infection. (A) Representative contour plots for Ly6G/Ly6C and F4/80/Ly6C, including gating strategy. Initially, neutrophils (Ly6G+) and Ly6G- cells were selected within CD11b+ cells. Afterwards, macrophages (F4/80+) and monocytes (Ly6C+F4/80-) were selected, within CD11b+Ly6G- cells. **(B)** Number of neutrophil per mg of tissue in spleen and gonadal AT. **(C)** Number of macrophages and monocytes per mg of tissue in spleen and gonadal AT. **(B-C)** Error bars represent the standard error of the mean (n=2-6 mice per group).

4.2.2. T cell subsets

4.2.2.1. Effector T cells

To determine if T cells recruited to AT produced an attenuated detrimental response against *T. brucei*, we analysed the dynamics of CD4+ and CD8+ T cell effectors, as defined by the surface markers CD3e+CD4+Foxp3- and CD3e+CD8+, respectively, that produced IFN-γ or TNF-α or co-produce these cytokines (see gating strategy in **Figure 8A**).

Throughout infection, the number of total CD4+ and CD8+ T cell subsets had similar behaviours, decreasing in the spleen and increasing in AT (**Supplementary figure 3**). Among the total pool of T cells, only a fraction gets activated, resulting in effector T cells. The numbers of effector CD4+ T cells and effector CD8+ T cells per mg of tissue decreased in the spleen, which can be explained by the increase of the spleen's mass. On the other hand, in gonadal AT, the number of effector CD4+ and CD8+ T cells per mg of tissue increased 64-fold and 38-fold, respectively (**Figure 8B and C**). The high expression of TNF-α and IFN-γ in gonadal AT (RNAseq unpublished data from our group) further confirm the steady accumulation of effector T cells in AT, which could result in parasite elimination. Given that AT is a site of parasite accumulation and not eradication, we tested the role of IFN-γ in parasite clearance *in vivo* by using IFN-γ-deficient mice and assessed the effect on *T. brucei* accumulation in the AT.

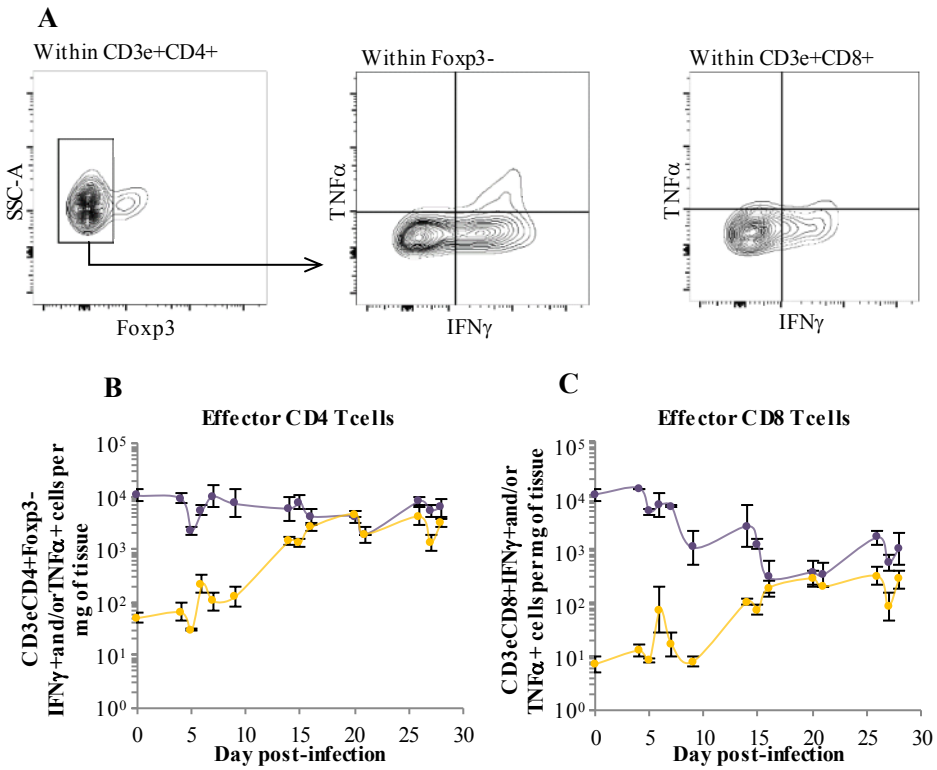

Figure 8. Dynamics of effector CD4 T cells and effector CD8 T cells throughout infection. **(A)** Representative contour plots for SSC-A/Foxp3 and TNFα/IFNγ, including gating strategy. Initially, Foxp3- cells were selected within CD3e+CD4+ cells. Afterwards, within Foxp3-, effector CD4 T cells (TNFα and/or IFNγ+) were selected using a quadrant notation. Finally, within CD3e+CD8+, effector CD8 T cells (TNFα and/or IFNγ+) were selected using a quadrant notation. **(B)** Number of effector CD4 T cells (TNFα and/or IFNγ+) per mg of tissue in spleen and gonadal AT **(C)** Number of effector CD8 T cells (TNFα and/or IFNγ+) per mg of tissue in spleen and gonadal AT. **(B-C)** Error bars represent the standard error of the mean. (n=2-6 mice per group).

4.2.2.1. Regulatory T cells

To determine if Treg cells are recruited to limit the effector T cell response, we analysed the dynamics of CD3e+CD4+Foxp3+ Treg cells (see gating strategy in **Figure 9A**). Throughout infection, in the same way, the numbers of Treg cells per mg of tissue decreased in the spleen. However, in gonadal AT, the numbers Treg cells per mg of tissue increased 21-fold. This suggests that Treg cells are recruited to AT and may have a counteractive effect, preventing the anti-*T. brucei* response (**Figure 9B**).

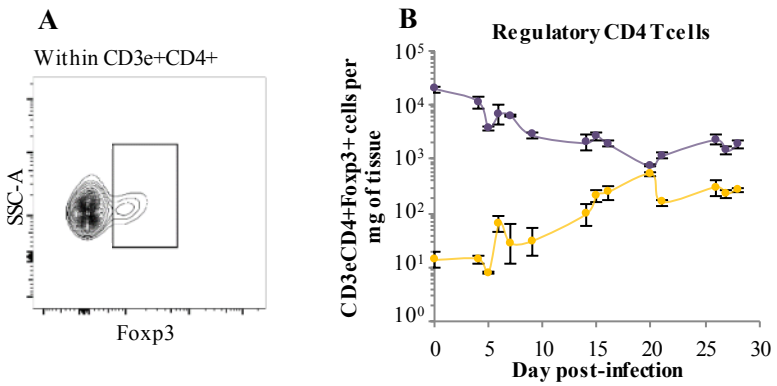

Figure 9. Dynamics of regulatory CD4 T cells throughout infection. **(A)** Representative contour plots for SSC-A/Foxp3. Regulatory CD4 T cells (Foxp3+) were selected within CD3e+CD4+ cells. **(B)** Number of regulatory CD4 T cells per mg of tissue in spleen and gonadal AT. Error bars represent the standard error of the mean (n=2-6 mice per group).

4.2.3. Immune checkpoints

Parasites often induce immunosuppression to reduce the capacity of the host to eliminate the infection[77–79]. To investigate if AT shows more signs of immunosuppression than other organs, we measured the expression of PD-1 and PD-L1 (see gating strategy in **Figure 10A**). From 0 to 28 dpi, we observed an increase in PD-1 expression in both CD4 and CD8 T cells to an extent of 9-fold and 12-fold in the spleen and 787-fold and 341-fold in gonadal AT, respectively (**Figure 10B and C**). This is accompanied by an increase in the expression of PD-L1, which binds to PD-1, to an extent of 2.5-fold in the spleen and 501-fold in gonadal AT (**Figure 10D**). If we consider number of cells per mg of tissue, PD-1/PD-L1 expression is globally higher in the systemic immune response than in the AT immune response. This is likely because the spleen is a major site of immune activation and the expression of such molecules prevents autoimmunity. However, when we consider the proportion of cells rather than the total number, we observe that the percentage of T cells that express PD-1 and the percentage of hematopoietic cells that express PD-L1 are higher in gonadal AT (**Figure 10E, F and G**). Strikingly, we observed a sharp increase from ~10 to ~70% of CD4 T cells and ~5 to ~30% of CD8 T cells expressing PD1 around 7-10 dpi, suggesting that this point of the infection may mark a progression from an early to a more chronic stage of the infection. Taken together, these results are consistent with the model that the PD-1/PD-L1 axis could potentially mediate higher levels of immunosuppression in gonadal AT than in spleen. This led us to test the role of PD-1 *in vivo* by using anti-PD-1 blocking antibody during infection and assess the effect on *T. brucei* accumulation in the AT.

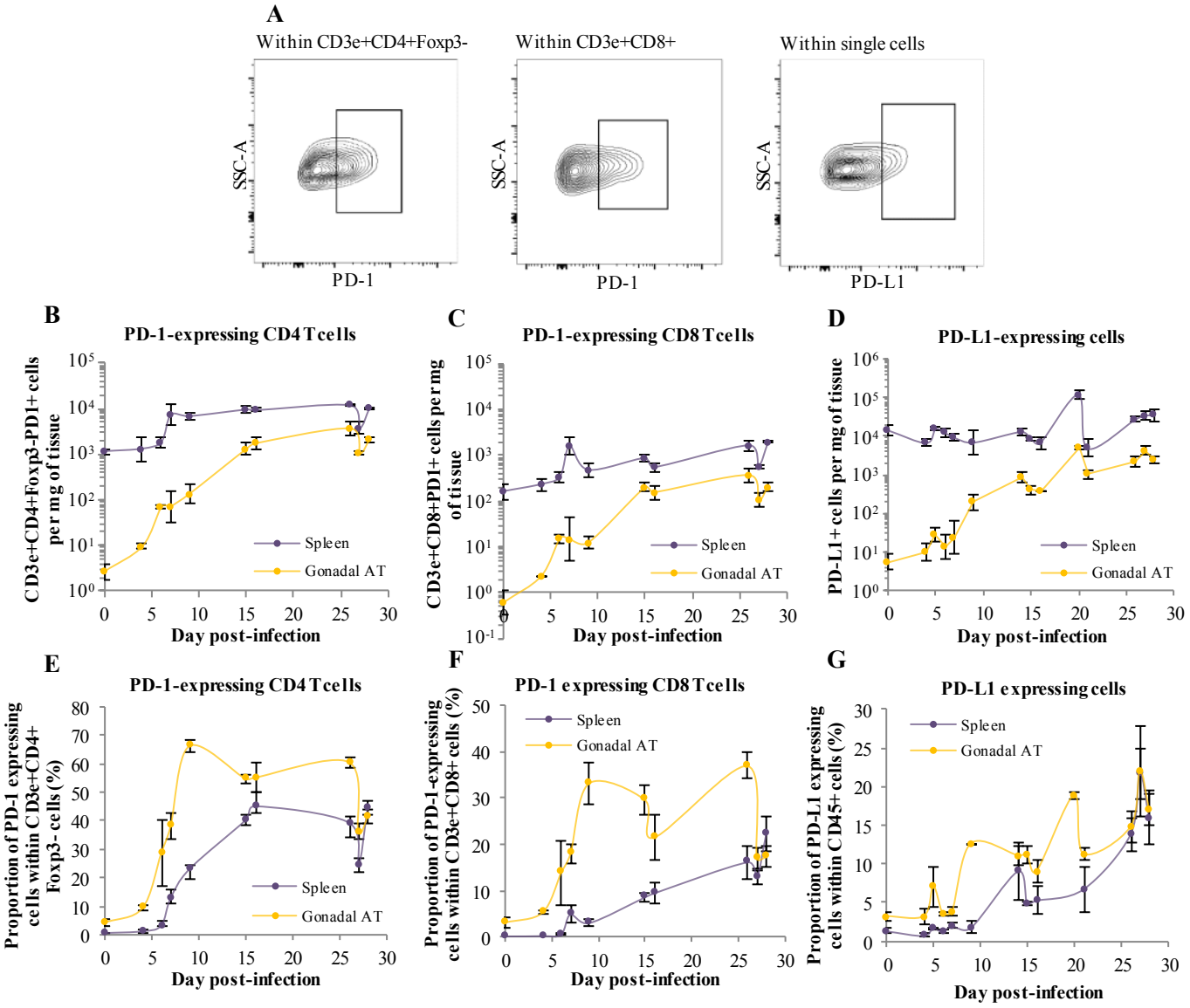

Figure 10. Dynamics of PD-1-expressing CD4 T cells and CD8 T cells and PD-L1-expressing cells throughout infection. **(A)** Representative contour plots for SSC-A/PD-1 and SSC-A/PD-L1, including gating strategy. PD-1-expressing CD4 T cells (PD-1+) were selected within CD3e+CD4+Foxp3- cells. PD-1-expressing CD8 T cells (PD-1+) were selected within CD3e+CD8+ cells. PD-L1 expressing cells (PD-L1+) were selected within single cells **(B)** Number of PD-1 expressing CD4 T cells per mg of tissue in spleen and gonadal AT. **(C)** Number of PD-1 expressing CD8 T cells per mg of tissue in spleen and gonadal AT. **(D)** Number of PD-L1 expressing cells per mg of tissue in spleen and gonadal AT. **(E)** Proportion of CD4 T cells that express PD-1 in spleen and gonadal AT. **(F)** Proportion of CD8 T cells that express PD-1 in spleen and gonadal AT. **(G)** Proportion immune (hematopoietic) cells that express PD-L1 in spleen and gonadal AT. **(B-G)** Error bars represent the standard error of the mean (n=2-6 mice per group).

4.3. Immune players in *T. brucei* persistence in adipose tissue

Considering the dynamics described above, two candidates that could be favouring parasite persistence in AT stood out. On one side, the increased production of IFN-γ in AT could be helping the parasite since this cytokine has been described as a growth stimulus for *T. brucei*[33,34]. On the other side, increased immunosuppression caused by engagement of PD-1 can lead to dysfunctional unresponsive T cells in AT. In this scenario, although T cells are recruited to AT, the parasite would not be eliminated. These hypotheses stand on the premise that these factors would be impairing parasite clearance in AT, and thus contribute for parasite accumulation in AT. To test these hypotheses, we first set out to understand if parasite clearance was dependent on adaptive immune response *in vivo*, then the influence of IFN-γ in parasite growth *in vitro* and in parasite clearance *in vivo* and, finally, the influence of PD-1/PD-L1 axis in parasite clearance *in vivo*.

In addition, resident IL-17-producing γδ T cells have also been described to regulate Treg cell homeostasis in AT[69]. Since Treg cells accumulate in gonadal AT, throughout infection, and might be beneficial for *T. brucei*, IL-17-producing γδ T cells could be favouring parasite persistence in this organ. Therefore, we tested the influence of γδ T cells and IL-17 in parasite clearance *in vivo*.

Finally, clearance of the first peak of parasitemia has been attributed mainly to anti-VSG IgMs, which are produced first and in high levels[49,50]. To understand whether clearance in AT also happens due to IgMs, we tested the importance of IgMs alone, without the influence of other isotypes, in parasite clearance *in vivo*.

Parasite clearance between 6 and 9 dpi was chosen as the timeframe for the experiments since, considering the dynamics of *T. brucei* infection, it is present in every infection in *wt* mice (**Figure 6A-C**). The high parasitemia and parasite numbers in both spleen and AT at 6 dpi, followed by the drop in the number of parasites and parasitemia at 9 dpi, gives us a window to study the effect of the above-mentioned factors in parasite clearance. Parasitemia was quantified by counting *T. brucei* numbers in a haemocytometer. The total number of *T. brucei* parasites in spleen, gonadal AT, heart and kidney were quantified by qPCR. Heart and kidney were used as a non-AT organs and non-lymphoid organs.

4.3.1. Lymphocytes in systemic and local parasite clearance

Between 6 and 9 dpi, parasites undergo clearance in blood, spleen and gonadal AT (**Figure 6A**). To establish if this clearance is dependent on adaptive immune response, we used mice deficient in recombination activation gene 2 (RAG2), which fail to generate mature T or B lymphocytes. Mice were infected with *T. brucei* and organs were collected at 6 and 9 dpi.

Following infection with *T. brucei*, RAG2-deficient mice display impaired parasite clearance in blood: parasitemia increases until 6 dpi and stabilises, failing to drop as observed in *wt* mice (**Figure 11A**). In the same way, between 6 and 9 dpi there is no parasite clearance in RAG2-deficient mice within the studied organs: spleen, gonadal AT and heart (**Figure 11B**). These results suggest that clearance from 6 to 9 dpi is dependent on adaptive immune response. Given the systemic effect of total absence of mature lymphocytes, the mechanism supporting preferential accumulation of the parasite in the AT cannot not be addressed in RAG2-deficient mice.

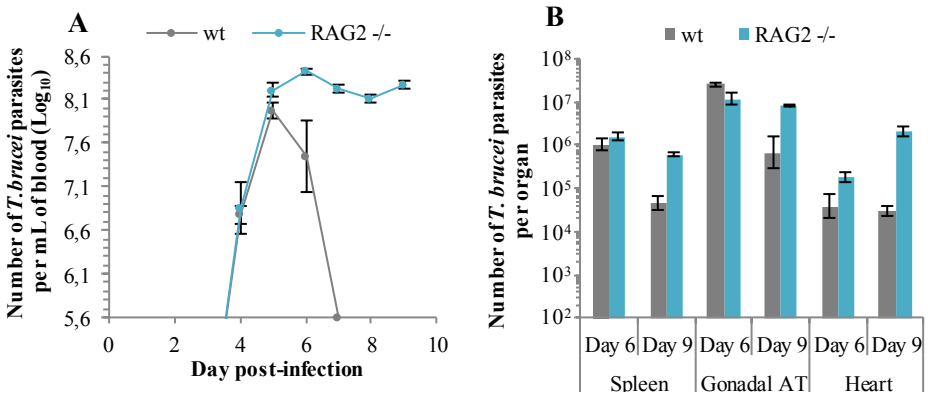

Figure 11. Systemic and local *T. brucei* clearance are dependent on adaptive immunity. (A-B) Infection of *wt* (grey) and RAG2-deficient (blue) mice with *T. brucei*. Error bars represent the standard error of the mean. (n=4 per group). **(A)** Parasitemia of mice infected with *T. brucei* (detection limit is 10^6 parasites per mL of blood). **(B)** Number of *T. brucei* parasites quantified by qPCR in spleen, gonadal AT and heart, 6 and 9 days after infection.

4.3.2. IFN-γ duality: parasite growth or parasite clearance?

Unexpectedly, IFN-γ has been described as both essential for control of infection[32,80] and a growth stimulus for *T. brucei*[33,34]. Therefore, considering the increased production of this cytokine in AT during infection, IFN-γ could be enhancing parasite growth, which would explain parasite accumulation. To assess if IFN-γ has a direct action as a growth factor, *T. brucei* growth was determined *in vitro*, in presence of varying concentrations of mouse IFN-γ, during 9 days. Dilution of the cultures were performed when necessary to ensure a parasite density below $5x10^5$ parasites/mL and avoid stumpy form differentiation. The presence of IFN-γ did not lead to an improvement in parasite growth, as fold-change per day was identical in all conditions (**Figure 12A**). This result indicates that IFN-γ does not have a direct beneficial effect in parasite growth *in vitro*.

Furthermore, to investigate whether IFN-γ improves proliferation *in vivo* and participate in the specific AT accumulation of the parasite, IFN-γ-deficient mice, which lack the production of this cytokine, were infected with *T. brucei* and organs were collected at 6 and 9 dpi.

After *T. brucei* infection, IFN-γ-deficient mice showed impaired parasite clearance. Contrary to blood of *wt* mice, parasitemia of IFN-γ-deficient mice increase until 6 dpi and stabilise, failing to clear (**Figure 12B**). In the same way, between 6 and 9 dpi there is no parasite clearance in the analysed organs: spleen, gonadal AT and heart (**Figure 12C**). Our results show that, in contrast to what has been previously proposed, IFN-γ does not appear to enhance parasite growth. Instead, it is necessary for systemic and local parasite clearance. Additionally, the similarity with the parasite clearance from RAG2- and IFN-γ-deficient mice suggests that the main effector function of T lymphocytes during *T. brucei* infection is IFN-γ production, supporting that clearance is a Th1-dependent response.

A

IFN-γ concentration (ng/mL)	Doubling time (hours)	Fold-increase per day
0	10,1	5,2
0.1	10	5,3
1	10,7	4,7
10	9,6	5,6
100	9,5	5,7

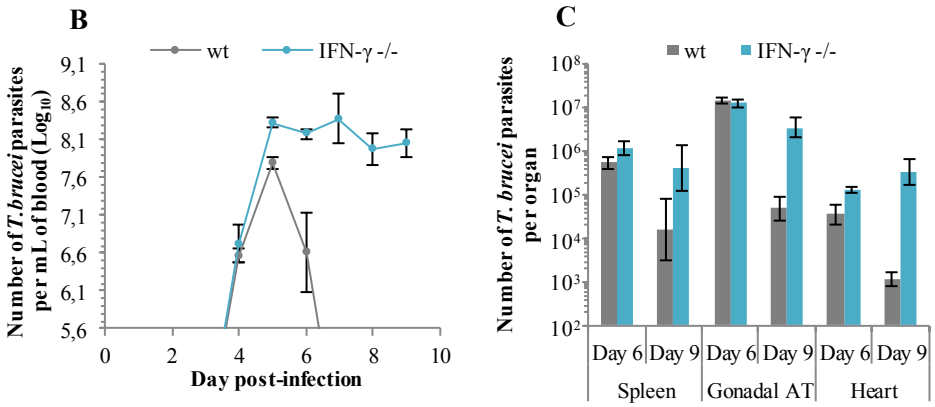

Figure 12. IFN-γ is essential for systemic and local *T. brucei* clearance. **(A)** Doubling time, in hours, and fold-increase per day of *T. brucei* parasites cultured *in vitro*, in the presence of murine IFN-γ. Parasite density was kept below $5x10^5$ parasites/mL to prevent differentiation. **(B-C)** Infection of *wt* (grey) and IFN-γ-deficient (blue) mice with *T. brucei*. Error bars represent the standard error of the mean. (n=4 per group). **(B)** Parasitemia of mice infected with *T. brucei.* **(C)** Number of *T. brucei* parasites quantified by qPCR in spleen, gonadal AT and heart, 6 and 9 days after infection.

4.3.3. PD-1-mediated T cell exhaustion in systemic and local parasite clearance

T. brucei may accumulate and persist in AT by taking advantage of a higher potential of PD1-mediated immunosuppression, which may limit T cell response and parasite elimination. The higher proportion of both PD-1 and PD-L1 expression in AT, throughout *T. brucei* infection (**Figure 10E, F and G**), led us to determine the importance of PD-1/PD-L1 in preventing parasite clearance. Mice were inoculated i.v. with PD-1-blocking antibody and infected with *T. brucei*, and organs were collected at 6 and 9 dpi.

By blocking the PD-1/PD-L1 axis *in vivo*, we expected a higher clearance of the parasite. However, when compared with non-inoculated wt mice, it had no significant effect in parasite clearance in blood, spleen and gonadal AT, between 6 and 9 dpi (**Figure 13**). This suggests that increased expression of PD-1/PD-L1 does not confer a more advantageous environment for the parasite to reside in AT, in early time-points.

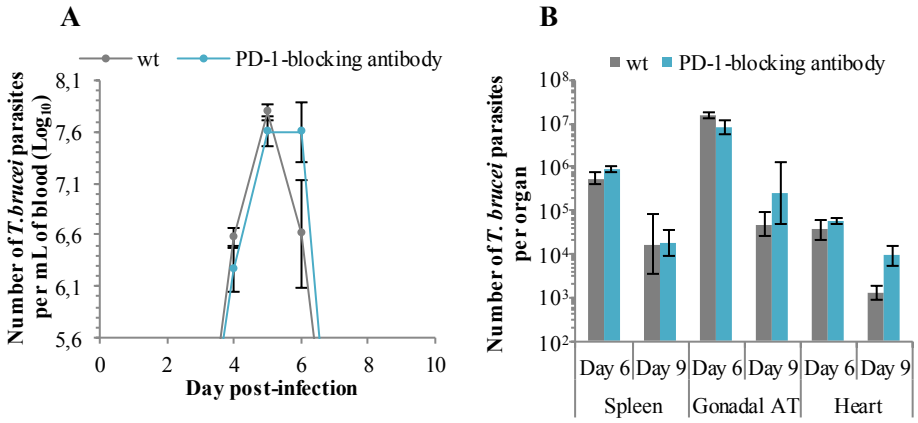

Figure 13. Increased PD-1/PD-L1 expression does not appear to contribute for *T. brucei* persistence in AT. (A-B) Infection with *T. brucei* of *wt* mice (grey) and *wt* mice inoculated i.v. with PD-1-blocking antibody (blue). Error bars represent the standard error of the mean. (n=4 per group). **(A)** Parasitemia of mice infected with *T. brucei*. **(B)** Number of *T. brucei* parasites quantified by qPCR in spleen, gonadal AT and heart, 6 and 9 days after infection.

4.3.4. γδ T cells and IL-17 in systemic and local parasite clearance

T. brucei may accumulate in AT by taking advantage of the presence of Treg cells that limit parasite elimination. Treg homeostasis in AT has been attributed to resident IL-17-producing γδ T cells[69], which could consequently impair parasite clearance. To determine the importance of resident IL-17-producing γδ T cells in parasite clearance, γδ T cell-deficient mice (TCRδ-/-) and IL-17-deficient mice were infected with *T. brucei* and organs were collected at 6 and 9 dpi.

Following infection with *T. brucei*, both γδ T cell-deficient and IL-17-deficient mice display regular parasite clearance in the blood (**Figure 14, Left**). However, in γδ T cell-deficient, between 6 and 9 dpi, there is an impaired parasite clearance in the spleen and no parasite clearance in gonadal AT and heart (**Figure 14A, Right**). This result suggests that γδ T cells are important for tissue parasite clearance, plausibly through their ability to produce IFN-γ. By contrast, in IL-17-deficient mice, no impairment of parasite clearance was observed in the studied organs: spleen, gonadal AT and heart (**Figure 14B, Right**). This result suggests that IL-17 expression does not have a role in parasite clearance from 6 to 9 dpi.

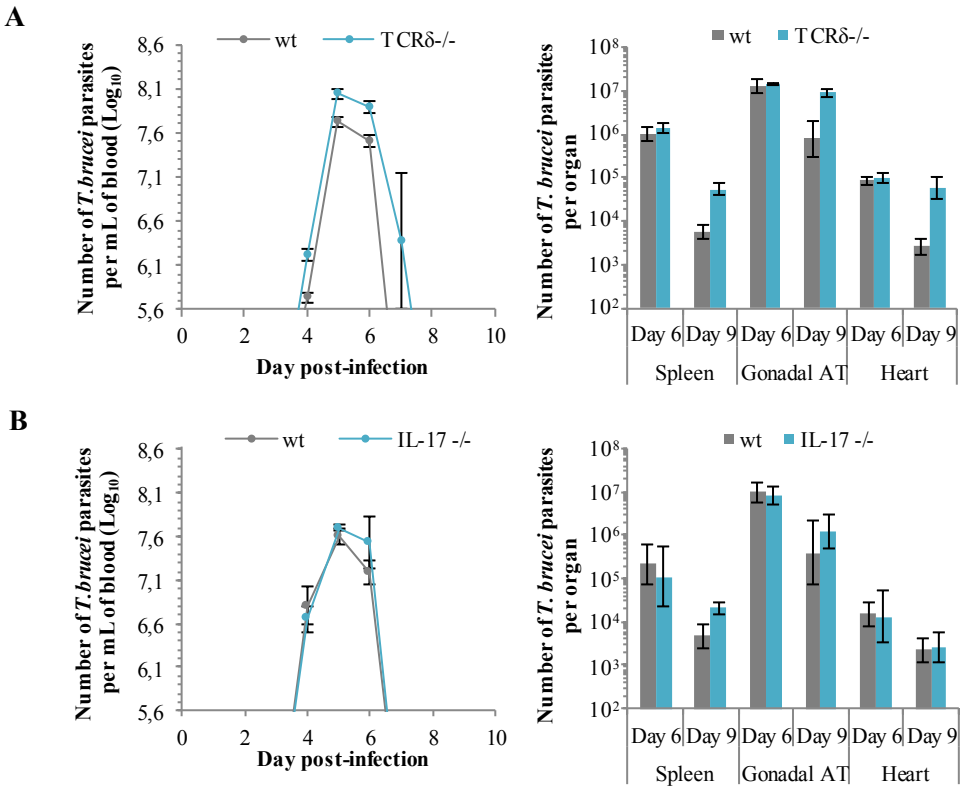

Figure 14. γδ T cells but not IL-17 are important in tissue *T. brucei* clearance. (A) Infection of *wt* (grey) and γδ T cell-deficient (blue) mice with *T. brucei*. **(B)** Infection of *wt* (grey) and IL-17-deficient (blue) mice with *T. brucei*. **(A,B)** Error bars represent the standard error of the mean. (n=3-4 per group). **(Left)** Parasitemia of mice infected with *T. brucei*. **(Right)** Number of *T. brucei* parasites quantified by qPCR in spleen, gonadal AT and heart, 6 and 9 days after infection.

4.3.5. IgMs in systemic and local parasite clearance

IgMs are key players in antibody-mediated parasite clearance in the blood[49,50]. Activation-induced cytidine deaminase (AID)-deficient mice lack the enzyme that triggers immunoglobulin isotype switching and affinity maturation. Consequently, IgMs do not undergo somatic hypermutation to increase their affinity, meaning that these mice only produce low-affinity IgMs and the other isotypes (IgG, IgA, IgE) are absent.

To dissect the role of IgM and IgG in parasite clearance in AT, AID-deficient mice were infected with *T. brucei* and organs were collected at 6, 9, 16 and 26 dpi. Following infection with *T. brucei*, AID-deficient mice show an identical parasitemia pattern as the *wt* mice, indicating that IgMs are sufficient to support parasite clearance in the blood (**Figure 15A**). In the same way, in spleen and kidney, the progression of parasite numbers from 6 to 26 dpi followed the same trend: parasite clearance between 6 to 9 dpi followed by an increase at 16 and 26 dpi (**Figure 15B**). Together, this suggests that the absence of other immunoglobulin isotypes and affinity maturation does not significantly affect parasite clearance systemically and in non-AT organs. Strikingly, in gonadal AT of AID-deficient mice, there was an impaired parasite clearance, failing to reduce the number of parasites between 6 and 9 dpi. From 9 to 16 dpi, although remaining higher than in *wt* mice, parasite number in AID-deficient mice underwent a 5-fold decrease. This reduction was then recovered from 16 to 26 dpi (**Figure 15B**).

Taken together, these results suggest that IgG, IgA and/or IgE are necessary for parasite clearance specifically in gonadal AT. This data also suggests that IgMs are insufficient to clear parasites in AT, but are sufficient to clear parasites in blood and spleen between 6 and 9 dpi. To further investigate this phenotype, we are currently developing the tools to measure the concentration of immunoglobulins in interstitial spaces of tissues.

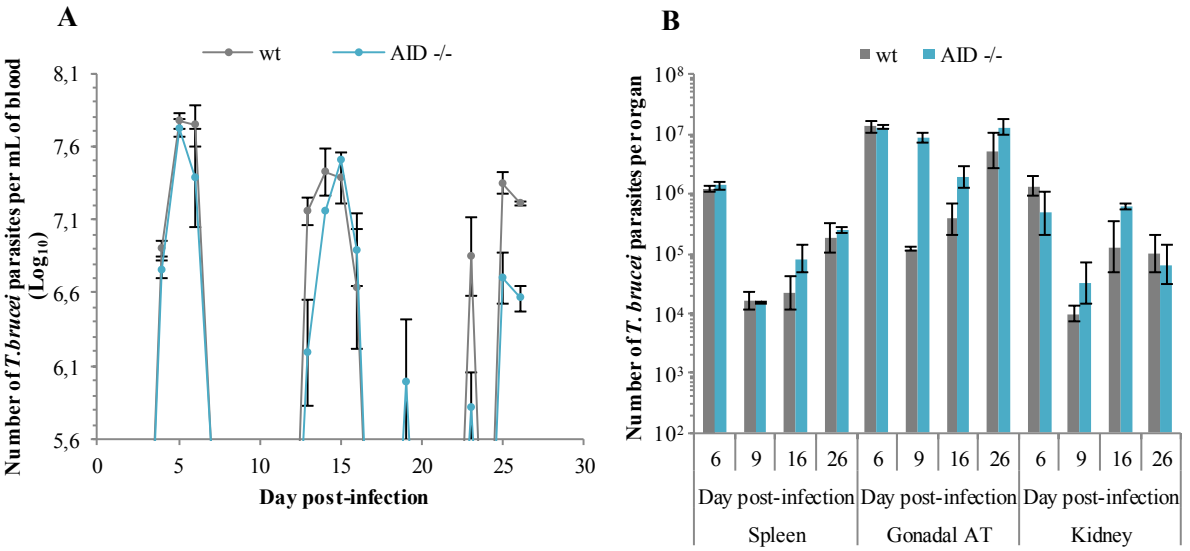

Figure 15. IgMs are not responsible for *T. brucei* clearance in gonadal AT. (A-B) Infection of *wt* (grey) and AID-deficient (blue) mice with *T. brucei.* Error bars represent the standard error of the mean. (n=2 per group). **(A)** Parasitemia of mice infected with *T. brucei*. **(B)** Number of *T. brucei* parasites quantified by qPCR in spleen, gonadal AT and kidney, 6, 9, 16 and 26 days after infection.

5. DISCUSSION AND FUTURE PERSPECTIVES

AT was recently found, by our laboratory, to be a main reservoir for *T. brucei* parasites in a mouse infection[9]. This discovery might challenge what we know regarding mechanisms of transmission, virulence and persistence in the host. In this work our aim was to identify factors (either from the parasite or the host) that benefit this tropism.

PARASITE FACTORS FAVORING ADIPOSE TISSUE TROPISM

In the first part of this project, we focused on the role of parasite metabolism in fat tropism, targeting three pathways: fatty acid β-oxidation, acetate production and oxidative phosphorylation.

TFEα has been previously predicted to have enoyl-CoA hydratase and 3-hydroxyacyl-CoA dehydrogenase enzymatic activities, making it a good candidate to catalyse the second and third step of β-oxidation[72,81]. This enzymatic activities had already been identified in *T. brucei* in biochemical assays[82]. In this work, we showed that the absence of this gene in *T. brucei* did not lead to an impairment in parasite accumulation in AT, both in early (6 dpi) and later (13 dpi) time-points. In addition, comparing with the parental cell line, no differences were observed in the parasitemia curve. Therefore, we can conclude that TFEα does not play a key role in the accumulation and persistence of *T. brucei* in AT. However, with these data, we cannot exclude β-oxidation as a pathway used by the parasite to persist in this organ. First, the encoding capacity of TFEα for the second and third steps of β-oxidation was based on an *in silico* prediction[72,81] and *in vitro* biochemical assays[82] and never confirmed experimentally *in vivo*. This means that other enzymes could be responsible for the enzymatic activities, necessary for fatty acid β-oxidation. Supporting this possibility, enoyl-CoA hydratase and 3-hydroxyacyl-CoA dehydrogenase activities were still observed in TFEα-deficient *T. brucei*, in PCF[72]. To confirm the presence/absence of such activities in TFEα-deficient ATF, enzymatic activity assays should be performed. In addition, to confirm if β-oxidation was impaired in TFEα-deficient ATF parasites, pulse-chase experiments with stable isotope-labelled fatty acid could be performed. However, currently, our efforts to impair β-oxidation shifted to a more promising candidate gene, maoC-like dehydratase, given that it is upregulated at the RNA level in ATF parasites. MaoC-like dehydratases have been shown to encode for enoyl-CoA hydratase activity, participating in the second step of β-oxidation, in other organisms such as *Escherichia coli* and *Pseudomonas aeruginosa*[83,84]. To this regard, we are currently generating maoC-like dehydratase deficient *T. brucei* parasites.

ASCT is the enzyme responsible for the conversion of acetyl-CoA to acetate, generating 1 ATP molecule by substrate phosphorylation, in PCF parasites[18]. This protein is upregulated in ATF parasites at the protein level (unpublished data from our laboratory). This upregulation could be the result of an adaptation, upon entry in AT, to route the acetyl-CoA produced in the active β-oxidation towards the production of energy. Our results showed, however, that ASCT-deficient *T. brucei* accumulates in gonadal AT as well as the parental *T. brucei* line, at an early time-point (5 dpi), reaching approximately 10^6 parasites per organ. Interestingly, the number of parasites in the heart reached the same value as gonadal AT, while the value normally attained is $3x10^4$ parasites per organ, at 5 dpi (for example: **Figure 5C**, bottom, heart, grey). It is our reasoning that hyperparasitemia at the moment of organ collection ($4x10^8$ parasites per mL of blood), which is near the mouse survival threshold, leads to an unspecific accumulation of parasites in non-AT organs. Although hyperparasitemia can pose a confounding factor, masking a reduced accumulation phenotype in gonadal AT, we have no reason to believe that unspecific accumulation of parasites happened in this organ, as parasite numbers did not surpass 10^6 parasites per

organ, which corresponds to the value normally attained in gonadal AT at 5 dpi (for example: **Figure 5C**, bottom, gonadal AT, grey). Therefore, with our data, there is no evidence that the upregulation of ASCT in ATF parasites favours accumulation and persistence in AT. If indeed *T. brucei* uses β-oxidation to produce energy, then acetyl-CoA is being routed elsewhere, for instance, the TCA cycle.

Finally, **NUBM** and **NUKM** are core proteins of complex I of the respiratory chain. Their successful deletion proved that electron transfer within complex I is not essential, highlighting their puzzling presence in BSF[85]. To this regard, complex I might be present in BSF parasites because, upon entry in AT, ATF parasites may use oxidative phosphorylation to produce energy, following β-oxidation and TCA cycle. Loss of either one of these proteins should render both complex I and respiratory chain inactive (Achim Schnaufer, personal communication). Contrary to expectation, we showed that the absence of each protein lead to strikingly different phenotypes regarding *T. brucei* accumulation in gonadal AT. While NUBM-deficient parasites accumulated 24-fold more, NUKM-deficient parasites accumulated 4-fold less than the parental cell line, in gonadal AT, at an early time-point (5 dpi). Of note, both mutants accumulated more in non-AT organs, to the same extent, when compared with the parental cell line.

Complex I has been suggested to participated in slender to stumpy form differentiation[86]. Accordingly, as mentioned before, our collaborator Achim Schnaufer described lack of slender to stumpy form differentiation in both mutants, which adds a significant confounding factor to our analysis, as these mutants develop hyperparasitemia contrary to the parental cell line. It is our reasoning that hyperparasitemia conducts to the increased accumulation of parasites in non-AT organs. In the same way, hyperparasitemia can also lead to the increased accumulation of parasites in gonadal AT infected with NUBM-deficient *T. brucei*. By contrast, NUKM-deficient *T. brucei*, even though displaying hyperparasitemia, lead to a decreased parasite burden in gonadal AT. It is plausible that in a fully pleomorphic background, that normally lacks hyperparasitemia, the absence of NUKM would generate an even more dramatic reduction in the number of parasites in the AT.

Why NUBM- and NUKM-deficient *T. brucei* parasites gave different phenotypes is a matter of speculation, as in fact the assembly of complex I of *T. brucei* is still being elucidated[85,87]. Nonetheless, our data reveals a possible role for NUKM in the accumulation and persistence of ATF parasites, most probably allowing energy production through oxidative phosphorylation. To further investigate this phenotype, we are currently generating new NUBM- and NUKM-deficient parasites in a confirmed fully pleomorphic background, to further confirm the involvement of NUKM in fat tropism.

Overall, in this part of the work, we identified NUKM as the most promising candidate that is specifically required for accumulation of parasites in the AT. Other experiments will be necessary to confirm the involvement of oxidative phosphorylation chain or, whether NUKM plays another yet unidentified role in *T. brucei*. It is important to note that, for practical reasons, in most of our experiments, we focused on an early time point of infection (days 5-6 post-infection) and our read out of number of parasites is qPCR of genomic DNA. It is possible that a reduction in tissue tropism takes longer to be detected. Therefore, we could consider scoring parasite load after 20 days of infection, quantify RNA (instead of DNA) and also test if there is an overall change in mouse survival.

HOST FACTORS FAVORING TISSUE TROPISM

In the second part of this project, we focused on the role of the local immune response against *T. brucei* in AT and immune players that potentially favour *T. brucei* persistence in this tissue.

Myeloid cells, especially macrophages, play a major role in the immune response against *T. brucei*, phagocyting opsonised parasites and releasing pro-inflammatory cytokines. In this work, we observed that monocytes/macrophages and neutrophils are promptly recruited to the AT and their number increases gradually with time. However, the functional nature of these macrophages and neutrophils was not assessed. Thus, it is not clear if the presence of these cells in AT implies an anti-*T. brucei* response, as protective roles have also been reported in *Trypanosoma cruzi*, another protozoan parasite that accumulates in AT[88]. In a mouse infection, *T. cruzi* induces neutrophils to become anti-inflammatory, produce IL-10 and downregulate IFN-γ release[89]. Furthermore, the induction of M2-like macrophages triggered by *T. cruzi* has been suggested to contribute for tissue homeostasis and parasite survival[90]. To understand the function of these cells in *T. brucei* infected AT, it is necessary to determine macrophage and neutrophil polarization. To do so, we envisage to purify macrophages and neutrophils by cell sorter associated flow cytometry and assess gene expression of specific markers that are exclusively related to the pro-inflammatory (TNF-α, IL-1β, IL-6, for example[91,92]) and anti-inflammatory phenotypes (arginase I, mannose receptor, Ym1 and TGF-β, for example[91,92]).

T cells are key players in the control of *T. brucei* infection. CD4 and CD8 effector T cells promote an immune response that acts to eliminate parasites, in large part through the production of IFN-γ and TNF-α. In this work, we showed that, throughout infection, both effector T cell subsets accumulate in AT, suggesting no restriction in recruitment of these cells. We predict that these cells express IFN-γ and TNF-α and eliminate *T. brucei*. Furthermore, we also observed that T cell accumulation was detectable from 6 dpi onwards, which fits with the delay necessary to establish an adaptive immune response.

The role of **IFN-γ** in *T. brucei* infection has been subject of controversy, as it was reported to be essential for resistance against infection[32,80] but also to act as a growth stimulus[33,34]. In this work, we first showed that IFN-γ does not appear to have a direct effect in *T. brucei* growth, *in vitro*. The inability to replicate the reported direct growth-stimulating effect, *in vitro*, might arise from the difference in the used methods. Bakhiet *et al*[34] determined growth rate in a one-time incubation of *T. brucei* with IFN-γ, during 16-20h. In contrast, we incubated *T. brucei* in the presence of IFN-γ, for 9 days, and the growth rate was calculated using a cumulative growth curve. Furthermore, *in vivo*, we showed that IFN-γ does not favour parasite proliferation but rather is essential for its elimination, as parasite clearance is reduced in blood, spleen and gonadal AT of IFN-γ-deficient mice. This is in agreement with what was previously reported[32]. Similar results were obtained with RAG2-deficient mice, suggesting that IFN-γ is mainly produced by cells of the adaptive immune response. Thus, although IFN-γ has been reported as a growth stimulus for *T. brucei*, our data reveals no evidence of such beneficial effect, meaning it is not a contributor for *T. brucei* accumulation and persistence in AT.

TNF-α is a well-known key player in the control of *T. brucei* infection. Therefore, the observed high expression of this cytokine in gonadal AT is likely to be deleterious for the parasite. However, TNF-α might have the contrary effect, as this cytokine was reported to stimulate lipolysis in human adipocytes[93]. It is conceivable that TNF-α triggers lipolysis, leading to an increased secretion of fatty acids by adipocytes, which could be imported and catabolized by β-oxidation by the parasite. Therefore, to understand if TNF-α contributes for *T. brucei* persistence in AT, we will infect TNF-α-deficient mice and determine parasite accumulation in gonadal AT.

PD-1 mediated T cell exhaustion leads to a weakened immune response against protozoan infections, such as *Plasmodium*, *Toxoplasma* and *Leishmania*[77–79]. The role of such immunosuppression in AT has never been addressed. In this work, we showed that the proportion of T cells that express PD-1 and the proportion of hematopoietic cells that express PD-L1 concomitantly increased in AT more than in the spleen, suggesting that the AT could be a highly immunosuppressed environment. However, when we blocked *in vivo* the PD-1/PD-L1 axis, parasites accumulated to the same extent than mice non-

treated with this checkpoint blocker. These results suggest that the higher expression of the PD-1/PD-L1 axis is not the molecular mechanism (local immunosuppression) that supports accumulation of the parasite in AT, at early time-points. It is possible however that the antibody blockade was ineffective, which would compromise these conclusions. Finally, we cannot exclude that the PD1/PD-L1 axis has a role in later time-points.

Treg cells are associated with poor control of *T. brucei* infection, by suppressing the protective response against the parasite[94]. In addition, Treg cells constitute an important population of cells in AT that contributes to an anti-inflammatory environment in this tissue. In this work, we showed that, during *T. brucei* infection, Treg cells accumulate in AT to a higher degree than in spleen from 6 dpi onwards. Further studies are required to assess the specific role of Treg cells in AT during infection. To understand if Treg cells in AT favour the presence of *T. brucei*, we are planning to use a mouse model that expresses the diphtheria toxin receptor upon control of Foxp3 (the master transcription factor of the development and differentiation of Treg cells), in which Treg cells can be depleted upon administration with diphtheria toxin[95,96]. These mouse model permits a targeted Treg depletion from a specific time-point onwards, allowing us to test both early and later Treg cell contributions.

Treg homeostasis in AT was reported to be regulated by a resident population of IL-17 producing γδ T cells. Thus, the potentially permissive immune response elicited by Treg cells could be an indirect effect of this subset of γδ T cells. We showed, however, that neither γδ T cells nor IL-17 contribute to *T. brucei* accumulation in AT. Interestingly, our data also suggests that γδ T cells are important for tissue clearance of parasites, as γδ T cell-deficient mice failed to clear *T. brucei* between 6 and 9 dpi in the assessed tissues (spleen, heart and gonadal AT). Since this impaired clearance was not specific to AT, no further investigation of this phenotype is planned. Nevertheless, once this studies move to a more representative model for AAT, such as cows, the effect of γδ T cells in the persistence of *T. brucei* in AT should be revisited, as the immune system of cattle contains a higher percentage of these cells when compared with humans and mice[97].

IgMs have been attributed to a pivotal role in the control of infection, by allowing antibody-mediated clearance. However, until now, it was not known whether this role extended to AT. We showed, in AID-deficient mice infections, that, although low-affinity IgMs are sufficient to clear the parasite in the blood, spleen and non-AT organs, no clearance happened in gonadal AT. Thus, for clearance in AT, other immunoglobulin isotypes are essential. The lower parasite burden in a later time-point (16 dpi) suggests that other factors, besides antibodies, might be involved in the clearance in gonadal AT.

Why IgMs are non-functional in AT is still under investigation. We have considered the following hypotheses. A possible scenario is that IgMs have an impaired function in AT due to reduced accessibility, as opposed to other isotypes of immunoglobulins. A selectively reduced concentration of IgMs in AT could happen either because IgMs in circulation, being pentamers (as opposed to IgA dimers and IgG monomers), do not enter the AT or because B cells in AT produce less IgMs. To understand if this is the case, we are currently quantifying IgM and IgG in the serum and AT by ELISA. Other possibilities are related to functionalities of the IgMs in AT. First, IgMs could bind poorly to ATF parasites, when compared to BSF parasites, leading to reduced complement- and/or macrophage-mediated elimination in AT. This could happen, for instance, due to local altered IgM glycosylation that may negatively affect complement- and/or macrophage- response(s), giving advantage to the parasite. The impact of glycosylation on the half-life of immunoglobulins and complement activation has already been addressed in the context of bacterial infections[98]. On the other hand, ATF parasites could secrete/express factors capable of altering the complement cascade or macrophage functions, rendering IgMs inefficient for parasite elimination in the AT. An example of such factor is the surface protease gp63. This protease has been shown to confer resistance to complement-mediated lysis in *Leishmania*

parasites[99] and functional homologues have been found in *T. brucei*[100,101]. Thus, such molecule may be an important virulence factor and should be assessed in the AT. Finally, selective and excessive presence of sVSG could act as an evasion mechanism to deplete anti-VSG IgMs in AT, thus limiting parasite elimination[25].

With this work, we have established several possibilities for immune players that might favour *T. brucei* accumulation in AT. Immunosuppression needs to be further investigated before eliminating this mechanism as a contributor to fat tropism. Currently, the most promising immune player are B cells, especially the impaired function of IgMs in AT. Overall, this work was the stepping stone to understand why *T. brucei* accumulates in AT.

6. REFERENCES

1. Simarro, P. P. *et al.* Estimating and Mapping the Population at Risk of Sleeping Sickness. *PLoS Negl. Trop. Dis.* **6,** e1859 (2012).
2. World Health Organization. Control and surveillance of human African trypanosomiasis. *World Health Organ. Tech. Rep. Ser.* 1–237 (2013).
3. Kennedy, P. G. E. Clinical features, diagnosis, and treatment of human African trypanosomiasis (sleeping sickness). *Lancet Neurol.* **12,** 186–194 (2013).
4. Kennedy, P. G. E. Human African trypanosomiasis-neurological aspects. *Journal of Neurology* **253,** 411–416 (2006).
5. Fairlamb, A. H. Chemotherapy of human African trypanosomiasis: Current and future prospects. *Trends in Parasitology* **19,** 488–494 (2003).
6. PAAT. On target against poverty: the Programme Against African Trypanosomiasis 1997–2007. *PAAT Inf. Serv. Publ.* (2008).
7. Vassella, E., Reuner, B., Yutzy, B. & Boshart, M. Differentiation of African trypanosomes is controlled by a density sensing mechanism which signals cell cycle arrest via the cAMP pathway. *J. Cell Sci.* **110,** 2661–2671 (1997).
8. Van Den Abbeele, J., Claes, Y., van Bockstaele, D., Le Ray, D. & Coosemans, M. Trypanosoma brucei spp. development in the tsetse fly: characterization of the post-mesocyclic stages in the foregut and proboscis. *Parasitology* **118,** 469–478 (1999).
9. Trindade, S. *et al.* Trypanosoma brucei Parasites Occupy and Functionally Adapt to the Adipose Tissue in Mice. *Cell Host Microbe* **19,** 837–848 (2016).
10. Capewell, P. *et al.* The skin is a significant but overlooked anatomical reservoir for vector-borne African trypanosomes. *Elife* **5,** (2016).
11. Van Hellemond, J. J., Bakker, B. M. & Tielens, A. G. M. *Energy metabolism and its compartmentation in Trypanosoma brucei*. *Advances in Microbial Physiology* **50,** (Elsevier Masson SAS, 2005).
12. Opperdoes, F. R. & Borst, P. Localization of nine glycolytic enzymes in a microbody-like organelle in Trypanosoma brucei: The glycosome. *FEBS Lett.* **80,** 360–364 (1977).
13. Visser, N., Opperdoes, F. R. & Borst, P. Subcellular Compartmentation of Glycolytic Intermediates in Trypanosoma brucei. *Eur. J. Biochem.* **118,** 521–526 (1981).
14. Szöör, B., Haanstra, J. R., Gualdrón-López, M. & Michels, P. A. M. Evolution, dynamics and specialized functions of glycosomes in metabolism and development of trypanosomatids. *Current Opinion in Microbiology* **22,** 79–87 (2014).
15. Helfert, S., Estévez, A. M., Bakker, B., Michels, P. & Clayton, C. Roles of triosephosphate isomerase and aerobic metabolism in Trypanosoma brucei. *Biochem. J.* **357,** 117–125 (2001).
16. Lamour, N. *et al.* Proline metabolism in procyclic Trypanosoma brucei is down-regulated in the presence of glucose. *J. Biol. Chem.* **280,** 11902–11910 (2005).
17. Van Weelden, S. W. H. *et al.* Procyclic Trypanosoma brucei do not use Krebs cycle activity for energy generation. *J. Biol. Chem.* **278,** 12854–12863 (2003).
18. Rivière, L. *et al.* Acetyl:succinate CoA-transferase in procyclic Trypanosoma brucei. Gene identification and role in carbohydrate metabolism. *J. Biol. Chem.* **279,** 45337–45346 (2004).
19. Mantilla, B. S. *et al.* Proline Metabolism is Essential for Trypanosoma brucei brucei Survival in the Tsetse Vector. *PLoS Pathog.* **13,** (2017).
20. Millerioux, Y. *et al.* The threonine degradation pathway of the Trypanosoma brucei procyclic form: The main carbon source for lipid biosynthesis is under metabolic control. *Mol. Microbiol.* **90,** 114–129 (2013).
21. Van Weelden, S. W. H., Van Hellemond, J. J., Opperdoes, F. R. & Tielens, A. G. M. New functions for parts of the krebs cycle in procyclic Trypanosoma brucei, a cycle not operating as a cycle. *J. Biol. Chem.* **280,** 12451–12460 (2005).
22. Geiger, A. *et al.* Escaping deleterious immune response in their hosts: Lessons from trypanosomatids. *Front. Immunol.* **7,** 1–21 (2016).
23. Akira, S., Uematsu, S. & Takeuchi, O. Pathogen recognition and innate immunity. *Cell* **124,** 783–801 (2006).

24. Thomas, C. J. & Schroder, K. Pattern recognition receptor function in neutrophils. *Trends in Immunology* **34,** 317–328 (2013).
25. Magez, S. *et al.* The glycosyl-inositol-phosphate and dimyristoylglycerol moieties of the glycosylphosphatidylinositol anchor of the trypanosome variant-specific surface glycoprotein are distinct macrophage-activating factors. *J. Immunol.* **160,** 1949–56 (1998).
26. Drennan, M. B. *et al.* The Induction of a Type 1 Immune Response following a Trypanosoma brucei Infection Is MyD88 Dependent. *J. Immunol.* **175,** 2501–2509 (2005).
27. Harris, T. H., Mansfield, J. M. & Paulnock, D. M. CpG oligodeoxynucleotide treatment enhances innate resistance and acquired immunity to African trypanosomes. *Infect. Immun.* **75,** 2366–2373 (2007).
28. Abdallah, D. S. A. *et al.* Toxoplasma gondii triggers release of human and mouse neutrophil extracellular traps. *Infect. Immun.* **80,** 768–777 (2012).
29. Baker, V. S. *et al.* Cytokine-associated neutrophil extracellular traps and antinuclear antibodies in Plasmodium falciparum infected children under six years of age. *Malar. J.* **7,** 41 (2008).
30. Guimarães-Costa, A. B. *et al.* Leishmania amazonensis promastigotes induce and are killed by neutrophil extracellular traps. *Proc. Natl. Acad. Sci. U. S. A.* **106,** 6748–6753 (2009).
31. Baetselier, P. D. *et al.* Alternative versus classical macrophage activation during experimental African trypanosomosis. *Int J Parasitol* **31,** 575–587 (2001).
32. Namangala, B., Noël, W., De Baetselier, P., Brys, L. & Beschin, a. Relative contribution of interferon-gamma and interleukin-10 to resistance to murine African trypanosomosis. *J. Infect. Dis.* **183,** 1794–800 (2001).
33. Olsson, T. *et al.* CD8 is critically involved in lymphocyte activation by a *T. brucei* brucei-released molecule. *Cell* **72,** 715–727 (1993).
34. Bakhiet, M. *et al.* Human and rodent interferon-γ as a growth factor for Trypanosoma brucei. *Eur. J. Immunol.* **26,** 1359–1364 (1996).
35. Magez, S. *et al.* Specific uptake of tumor necrosis factor-alpha is involved in growth control of Trypanosoma brucei. *J. Cell Biol.* **137,** 715–727 (1997).
36. Magez, S. *et al.* Tumor Necrosis Factor Alpha Is a Key Mediator in the Regulation of Experimental Trypanosoma brucei Infections. *Infect Immun* **67,** 3128–3132 (1999).
37. Salmon, D. *et al.* Adenylate Cyclases of Trypanosoma brucei Inhibit the Innate Immune Response of the Host. *Science (80-.).* **337,** 463–466 (2012).
38. Guilliams, M. *et al.* Experimental expansion of the regulatory T cell population increases resistance to African trypanosomiasis. *J. Infect. Dis.* **198,** 781–791 (2008).
39. Keir, M. E., Butte, M. J., Freeman, G. J. & Sharpe, A. H. PD-1 and Its Ligands in Tolerance and Immunity. *Annu. Rev. Immunol.* **26,** 677–704 (2008).
40. Oka, M., Ito, Y., Furuya, M. & Osaki, H. Trypanosoma gambiense: Immunosuppression and polyclonal B-cell activation in mice. *Exp. Parasitol.* **58,** 209–214 (1984).
41. Buza, J., Sileghem, M., Gwakisa, P. & Naessens, J. CD5+ B lymphocytes are the main source of antibodies reactive with non-parasite antigens in Trypanosoma congolense-infected cattle. *Immunology* **92,** 226–233 (1997).
42. Shoda, L. K. M. *et al.* DNA from protozoan parasites Babesia bovis, Trypanosoma cruzi, and *T. brucei* is mitogenic for B lymphocytes and stimulates macrophage expression of interleukin-12, tumor necrosis factor alpha, and nitric oxide. *Infect. Immun.* **69,** 2162–2171 (2001).
43. Diffley, P. Trypanosomal surface coat variant antigen causes polyclonal lymphocyte activation. *J. Immunol.* **131,** 1983–6 (1983).
44. Kobayakawa, T., Louis, J., Izui, S. & Lambert, P.-H. Autoimmune Response to DNA, Red Blood Cells, and Thymocyte Antigens in Association with Polyclonal Antibody Synthesis During Experimental African Trypanosomiasis. *J. Immunol.* **122,** (1979).
45. Buza, J. & Naessens, J. Trypanosome non-specific IgM antibodies detected in serum of Trypanosoma congolense-infected cattle are polyreactive. *Vet. Immunol. Immunopathol.* **69,** 1–9 (1999).
46. Magez, S. *et al.* The role of B-cells and IgM antibodies in parasitemia, anemia, and VSG switching in Trypanosoma brucei-infected mice. *PLoS Pathog.* **4,** (2008).
47. Reinitz, D. M. & Mansfield, J. M. T-cell-independent and T-cell-dependent B-cell responses to exposed variant surface glycoprotein epitopes in trypanosome-infected mice. *Infect. Immun.* **58,**

2337–2342 (1990).
48. Morrison, W. I., Black, S. J., Paris, J., Hinson, C. A. & Wells, P. W. Protective immunity and specificity of antibody responses elicited in cattle by irradiated Trypanosoma brucei. *Parasite Immunol.* **4,** 395–407 (1982).
49. Radwanska, M. *et al.* Comparative analysis of antibody responses against HSP60, invariant surface glycoprotein 70, and variant surface glycoprotein reveals a complex antigen-specific pattern of immunoglobulin isotype switching during infection by Trypanosoma brucei. *Infect. Immun.* **68,** 848–860 (2000).
50. Levine, R. F. & Mansfield, J. M. Genetics of resistance to the African trypanosomes. III. Variant-specific antibody responses of H-2-compatible resistant and susceptible mice. *J. Immunol. (Baltimore, Md 1950)* **133,** 1564–1569 (1984).
51. Reinitz, D. M. & Mansfield, J. M. Independent regulation of B cell responses to surface and subsurface epitopes of African trypanosome variable surface glycoproteins. *J Immunol* **141,** 620–626 (1988).
52. Stijlemans, B. *et al.* Efficient targeting of conserved cryptic epitopes of infectious agents by single domain antibodies: African trypanosomes as paradigm. *J. Biol. Chem.* **279,** 1256–1261 (2004).
53. Horn, D. Antigenic variation in African trypanosomes. *Molecular and Biochemical Parasitology* **195,** 123–129 (2014).
54. MacGregor, P., Savill, N. J., Hall, D. & Matthews, K. R. Transmission stages dominate trypanosome within-host dynamics during chronic infections. *Cell Host Microbe* **9,** 310–318 (2011).
55. Mugnier, M. R., Cross, G. A. M. & Papavasiliou, F. N. The in vivo dynamics of antigenic variation in Trypanosoma brucei. *Science (80-.).* **347,** 1470–1473 (2015).
56. Ahima, R. S. & Flier, J. S. Adipose tissue as an endocrine organ. *Trends Endocrinol. Metab.* **11,** 327–332 (2000).
57. Grant, R. W. & Dixit, V. D. Adipose tissue as an immunological organ. *Obesity* **23,** 512–518 (2015).
58. Teixeira, L. *et al.* Immune response in the adipose tissue of lean mice infected with the protozoan parasite Neospora caninum. *Immunology* **145,** 242–257 (2015).
59. Bapat, S. P. *et al.* Depletion of fat-resident Treg cells prevents age-associated insulin resistance. *Nature* **528,** 137–41 (2015).
60. Lumeng, C. N., Bodzin, J. L. & Saltiel, A. R. Obesity induces a phenotypic switch in adipose tissue macrophage polarization. *J. Clin. Invest.* **117,** 175–184 (2007).
61. Sun, K., Kusminski, C. M. & Scherer, P. E. Adipose tissue remodeling and obesity. *Journal of Clinical Investigation* **121,** 2094–2101 (2011).
62. Zaragosi, L.-E. *et al.* Activin a plays a critical role in proliferation and differentiation of human adipose progenitors. *Diabetes* **59,** 2513–21 (2010).
63. Orr, J. S. *et al.* Obesity alters adipose tissue macrophage iron content and tissue iron distribution. *Diabetes* **63,** 421–432 (2014).
64. Nguyen, K. D. *et al.* Alternatively activated macrophages produce catecholamines to sustain adaptive thermogenesis. *Nature* **480,** 104–108 (2011).
65. Odegaard, J. I. *et al.* Macrophage-specific PPARγ controls alternative activation and improves insulin resistance. *Nature* **447,** 1116–1120 (2007).
66. Rosen, E. D. *et al.* PPARγ is required for the differentiation of adipose tissue in vivo and in vitro. *Mol. Cell* **4,** 611–617 (1999).
67. Kosteli, A. *et al.* Weight loss and lipolysis promote a dynamic immune response in murine adipose tissue. *J. Clin. Invest.* **120,** 3466–3479 (2010).
68. Feuerer, M. *et al.* Lean, but not obese, fat is enriched for a unique population of regulatory T cells that affect metabolic parameters. *Nat. Med.* **15,** 930–939 (2009).
69. Kohlgruber, A. C., Gal-oz, S., Lamarche, N. M., Duquette, D. & Hung, N. γδ T cells producing IL-17A regulate adipose Treg homeostasis and thermogenesis. *Unpublished*
70. Engstler, M. & Boshart, M. Cold shock and regulation of surface protein trafficking convey sensitization to inducers of stage differentiation in Trypanosoma brucei. *Genes Dev.* **18,** 2798–2811 (2004).

71. Johnson, J. G. & Cross, G. A. Selective cleavage of variant surface glycoproteins from Trypanosoma brucei. *Biochem. J.* **178,** 689–97 (1979).
72. Allmann, S. *et al.* Triacylglycerol storage in lipid droplets in procyclic trypanosoma brucei. *PLoS One* **9,** e114628 (2014).
73. Hirumi, H. & Hirumi, K. Continuous Cultivation of Trypanosoma brucei Blood Stream Forms in a Medium Containing a Low Concentration of Serum Protein without Feeder Cell Layers. *J. Parasitol.* **75,** 985 (1989).
74. Schumann Burkard, G., Jutzi, P. & Roditi, I. Genome-wide RNAi screens in bloodstream form trypanosomes identify drug transporters. *Mol. Biochem. Parasitol.* **175,** 91–94 (2011).
75. Wolfensohn, S. & Llyod, M. *Handbook of laboratory animal management and welfare*. *The Canadian Veterinary Journal* **41,** (2003).
76. Bronte, V. & Pittet, M. J. The spleen in local and systemic regulation of immunity. *Immunity* **39,** 806–818 (2013).
77. Butler, N. S. *et al.* Therapeutic blockade of PD-L1 and LAG-3 rapidly clears established blood-stage Plasmodium infection. *Nat. Immunol.* **13,** 188–195 (2011).
78. Bhadra, R., Gigley, J. P., Weiss, L. M. & Khan, I. A. Control of Toxoplasma reactivation by rescue of dysfunctional CD8+ T-cell response via PD-1-PDL-1 blockade. *Proc. Natl. Acad. Sci.* **108,** 9196–9201 (2011).
79. Joshi, T., Rodriguez, S., Perovic, V., Cockburn, I. A. & Stäger, S. B7-H1 blockade increases survival of dysfunctional CD8+ T cells and confers protection against Leishmania donovaniinfections. *PLoS Pathog.* **5,** e1000431 (2009).
80. Hertz, C. J., Filutowicz, H. & Mansfield, J. M. Resistance to the African trypanosomes is IFN-gamma dependent. *J.Immunol.* **161,** 6775–6783 (1998).
81. Opperdoes, F. R. & Szikora, J. P. In silico prediction of the glycosomal enzymes of Leishmania major and trypanosomes. *Mol. Biochem. Parasitol.* **147,** 193–206 (2006).
82. Wiemer, E. A. C., IJlst, L., Van Roy, J., Wanders, R. J. A. & Opperdoes, F. R. Identification of 2-enoyl coenzyme A hydratase and NADP+-dependent 3-hydroxyacyl-CoA dehydrogenase activity in glycosomes of procyclic Trypanosoma brucei. *Mol. Biochem. Parasitol.* **82,** 107–111 (1996).
83. Park, S. J. & Lee, S. Y. Identification and characterization of a new enoyl coenzyme a hydratase involved in biosynthesis of medium-chain-length polyhydroxyalkanoates in recombinant Escherichia coli. *J. Bacteriol.* **185,** 5391–5397 (2003).
84. Tsuge, T. *et al.* Molecular cloning of two (R)-specific enoyl-CoA hydratase genes from Pseudomonas aeruginosa and their use for polyhydroxyalkanoate synthesis. *FEMS Microbiol. Lett.* **184,** 193–198 (2000).
85. Surve, S., Heestand, M., Panicucci, B., Schnaufer, A. & Parsons, M. Enigmatic presence of mitochondrial complex I in Trypanosoma brucei bloodstream forms. *Eukaryot. Cell* **11,** 183–193 (2012).
86. Bienen, E. J., Saric, M., Pollakis, G., Grady, R. W. & Clarkson, A. B. Mitochondrial development in Trypanosoma brucei brucei transitional bloodstream forms. *Mol. Biochem. Parasitol.* **45,** 185–192 (1991).
87. Duarte, M. & Tomás, A. M. The mitochondrial complex I of trypanosomatids - An overview of current knowledge. *Journal of Bioenergetics and Biomembranes* **46,** 299–311 (2014).
88. Combs, T. P. *et al.* The adipocyte as an important target cell for Trypanosoma cruzi infection. *J. Biol. Chem.* **280,** 24085–24094 (2005).
89. Boari, J. T. *et al.* IL-17RA signaling reduces inflammation and mortality during trypanosoma cruzi infection by recruiting suppressive IL-10-producing neutrophils. *PLoS Pathog.* **8,** e1002658 (2012).
90. Cabalén, M. E. *et al.* Chronic Trypanosoma cruzi infection potentiates adipose tissue macrophage polarization toward an anti-inflammatory M2 phenotype and contributes to diabetes progression in a diet-induced obesity model. *Oncotarget* **7,** 13400–15 (2016).
91. Penas, F. *et al.* Treatment in vitro with PPARα and PPARγ ligands drives M1-to-M2 polarization of macrophages from T. cruzi-infected mice. *Biochim. Biophys. Acta - Mol. Basis Dis.* **1852,** 893–904 (2015).
92. Ma, Y. *et al.* Temporal neutrophil polarization following myocardial infarction. *Cardiovasc. Res.*

110, 51–61 (2016).
93. Zhang, H. H., Halbleib, M., Ahmad, F., Manganiello, V. C. & Greenberg, A. S. Tumor necrosis factor-α stimulates lipolysis in differentiated human adipocytes through activation of extracellular signal-related kinase and elevation of intracellular cAMP. *Diabetes* **51,** 2929–2935 (2002).
94. Wei, G. & Tabel, H. Regulatory T Cells Prevent Control of Experimental African Trypanosomiasis. *J. Immunol.* **180,** 2514–2521 (2008).
95. Lahl, K. *et al.* Selective depletion of Foxp3 $^{+}$ regulatory T cells induces a scurfy-like disease. *J. Exp. Med.* **204,** 57–63 (2007).
96. Kim, J. M., Rasmussen, J. P. & Rudensky, A. Y. Regulatory T cells prevent catastrophic autoimmunity throughout the lifespan of mice. *Nat. Immunol.* **8,** 191–197 (2007).
97. Mackay, C. R. & Hein, W. R. A large proportion of bovine T cells express the γδ T cell receptor and show a distinct tissue distribution and surface phenotype. *Int. Immunol.* **1,** 540–545 (1989).
98. Wang, F. *et al.* Structural and functional characterization of glycosylation in an immunoglobulin G1 to Cryptococcus neoformans glucuronoxylomannan. *Mol. Immunol.* **43,** 987–998 (2006).
99. Brittingham, A. *et al.* Role of the Leishmania surface protease gp63 in complement fixation, cell adhesion, and resistance to complement-mediated lysis. *J. Immunol.* **155,** 3102–3111 (1995).
100. LaCount, D. J., Gruszynski, A. E., Grandgenett, P. M., Bangs, J. D. & Donelson, J. E. Expression and Function of the Trypanosoma brucei Major Surface Protease (GP63) Genes. *J. Biol. Chem.* **278,** 24658–24664 (2003).
101. El-Sayed, N. M. A. & Donelson, J. E. African trypanosomes have differentially expressed genes encoding homologues of the Leishmania GP63 surface protease. *J. Biol. Chem.* **272,** 26742–26748 (1997).

7. ANNEXES

7.1. Annex 1: Supplementary Tables

Supplementary table 1. Constructs provided by Dr. Frédéric Bringaud to knockout TFEα. Underline lowercase represents the targeting region. Uppercase represents the resistance gene.

Construct with PAC	aacttctgtgttgagatcgaaacggtgacagtttaaattcctttaatgaatggaagatatattataaaattgtgtggagaagtaatcaatgatgtggacgcatcatcatga cttgagttggcggcgacattttacacatttatttttttatcgctcgcaggtacgatgacgcgttgttagtgagaaacaatggatttaaaggacgcaacgtgaagggcggaaat ctgtgggatcggaggttgattggcggtagaaatttaacttttgttcgcgcgtgtgtgcggccacccttccacacaatgattccataacatcattgtacttttcttccttttggtaa tgtaagccgagttcgttgatacgtcagactctgtagtgtactgttttcggttgattacatgttctttatttggttttcatgttcacctgtctttttttttttgtgtgtgtgtgtcacgag gggtgtagcggctcatttttggaccaccgcttctggctgttcctgccatttatttgttaagagcaaagatacacagcttctagaATGACCGAGTACAAGCCC ACGGTGCGCCTCGCCACCCGCGACGACGTCCCCCGGGCCGTACGCACCCTCGCCGCCGCGTTCGCCGA CTACCCCGCCACGCGCCACACCGTCGACCCGGACCGCCACATCGAGCGGGTCACCGAGCTGCAAGAA CTCTTCCTCACGCGCGTCGGGCTCGACATCGGCAAGGTGTGGGTCGCGGACGACGGCGCCGCGGTGGC GGTCTGGACCACGCCGGAGAGCGTCGAAGCGGGGGCGGTGTTCGCCGAGATCGGCCCGCGCATGGCC GAGTTGAGCGGTTCCCGGCTGGCCGCGCAGCAACAGATGGAAGGCCTCCTGGCGCCGCACCGGCCCA AGGAGCCCGCGTGGTTCCTGGCCACCGTCGGCGTCTCGCCCGACCACCAGGGCAAGGGTCTGGGCAG CGCCGTCGTGCTCCCCGGAGTGGAGGCGGCCGAGCGCGCCGGGGTGCCCGCCTTCCTGGAGACCTCCG CGCCCCGCAACCTCCCCTTCTACGAGCGGCTCGGCTTCACCGTCACCGCCGACGTCGAGTGCCCGAAG GACCGCGCGACCTGGTGCATGACCCGCAAGCCCGGTGCCTGAaagctttttgacagtgttatgtgcagagaaggggagagaaaa gaaggaatgagggtaaaagaagaagagacgcgaggaacgaaatttttttaaaagaaggggggaggagttgggaggtataagtgaaataggatcgaaggtgaagagtca ctaaatcgcgtgcgtgtatccgcgtgcactgcgtttgttggtgtctgtgtactgtattgtggtagcgctctattacattcaaatgtttttttctatatatttttttaaaattacttttgttttctc ctctcactgatttgtcgttgttattatgagttccgttaattgacattatctttttttttttagaaagaagtttaggaaagggaggattcggtccgcgtgaacacatttaattatgcgaat atctccataggtatatgtacttggctggatgcgtgaatataccaatattgatcttcttgctcttcacttcgctattgtatgaccacactatttcgtt
Construct with BSD	aacttctgtgttgagatcgaaacggtgacagtttaaattcctttaatgaatggaagatatattataaaattgtgtggagaagtaatcaatgatgtggacgcatcatcatga cttgagttggcggcgacattttacacatttatttttttatcgctcgcaggtacgatgacgcgttgttagtgagaaacaatggatttaaaggacgcaacgtgaagggcggaaat ctgtgggatcggaggttgattggcggtagaaatttaacttttgttcgcgcgtgtgtgcggccacccttccacacaatgattccataacatcattgtacttttcttccttttggtaa tgtaagccgagttcgttgatacgtcagactctgtagtgtactgttttcggttgattacatgttctttatttggttttcatgttcacctgtctttttttttttgtgtgtgtgtgtcacgag gggtgtagcggctcatttttggaccaccgcttctggctgttcctgccatttatttgttaagagcaaagatacacagcttctagaATGGCCAAGCCTTTGTCTC AAGAAGAATCCACCCTCATTGAAAGAGCAACGGCTACAATCAACAGCATCCCCATCTCTGAAGACTA CAGCGTCGCCAGCGCAGCTCTCTCTAGCGACGGCCGCATCTTCACTGGTGTCAATGTATATCATTTTAC TGGGGGACCTTGTGCAGAACTCGTGGTGCTGGGCACTGCTGCTGCTGCGGCAGCTGGCAACCTGACTT GTATCGTCGCGATCGGAAATGAGAACAGGGGCATCTTGAGCCCCTGCGGACGGTGCCGACAGGTGCT TCTCGATCTGCATCCTGGGATCAAAGCCATAGTGAAGGACAGTGATGGACAGCCGACGGCAGTTGGG ATTCGTGAATTGCTGCCCTCTGGTTATGTGTGGGAGGGCTAAaagctttttgacagtgttatgtgcagagaaggggagagaaaag aaggaatgagggtaaaagaagaagagacgcgaggaacgaaatttttttaaaagaaggggggaggagttgggaggtataagtgaaataggatcgaaggtgaagagtcact aaatcgcgtgcgtgtatccgcgtgcactgcgtttgttggtgtctgtgtactgtattgtggtagcgctctattacattcaaatgtttttttctatatatttttttaaaattacttttgttttctcct ctcactgatttgtcgttgttattatgagttccgttaattgacattatctttttttttttagaaagaagtttaggaaagggaggattcggtccgcgtgaacacatttaattatgcgaatat ctccataggtatatgtacttggctggatgcgtgaatataccaatattgatcttcttgctcttcacttcgctattgtatgaccacactatttcgtt

Supplementary table 2. Primers used for TFEα knockout confirmation by PCR. The primers that target TFEα 5'-UTR and TFEα 3'-UTR anneal outside the targeting region.

Target	Primers	
	Forward	Reverse
TFEα	CCTTGTTTCCACTCCCTTGC	CCTATAGTGGGCTGCGAGTG
BSD	CGGCTACAATCAACAGCATC	ACGATACAAGTCAGGTTGCC
PAC	CACCGAGCTGCAAGAACT	GGCCTTCCATCTGTTGCTG
TFEα 5'-UTR	GACGGTGCAGTAGTGGTGAA	-
TFEα 3'-UTR	-	GCACCTCGGACAAGACTACT

7.2. Annex 2: Supplementary Figures

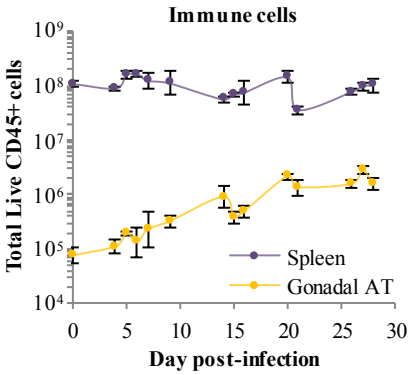

Supplementary figure 1. Dynamics of total immune cells throughout infection. Total number of immune cells (CD45+) in spleen and gonadal AT**.** Error bars represent the standard error of the mean. (n=2-6 mice per group).

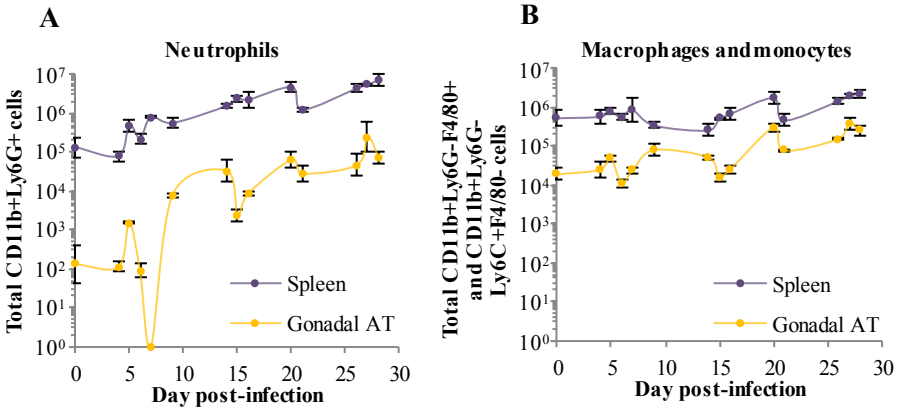

Supplementary figure 2. Dynamics of total neutrophils, macrophages and monocytes throughout infection. (A) Total number of neutrophils in spleen and gonadal AT. **(B)** Total number of macrophages and monocytes in spleen and gonadal AT. **(A-B)** Error bars represent the standard error of the mean (n=2-6 mice per group).

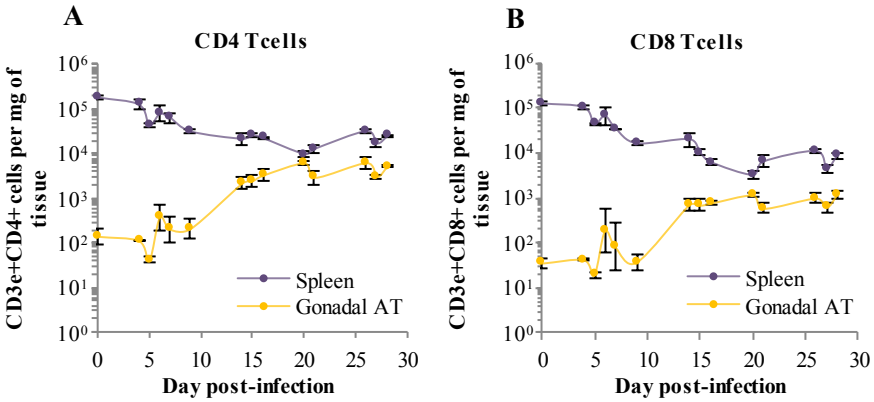

Supplementary figure 3. Dynamics of CD4 T cells and CD8 T cells throughout infection. (A) Number of CD4 T cells per mg of tissue in spleen and gonadal AT **(B)** Number of CD8 T cells per mg of tissue in spleen and gonadal AT. **(A-B)** Error bars represent the standard error of the mean. (n=2-6 mice per group).

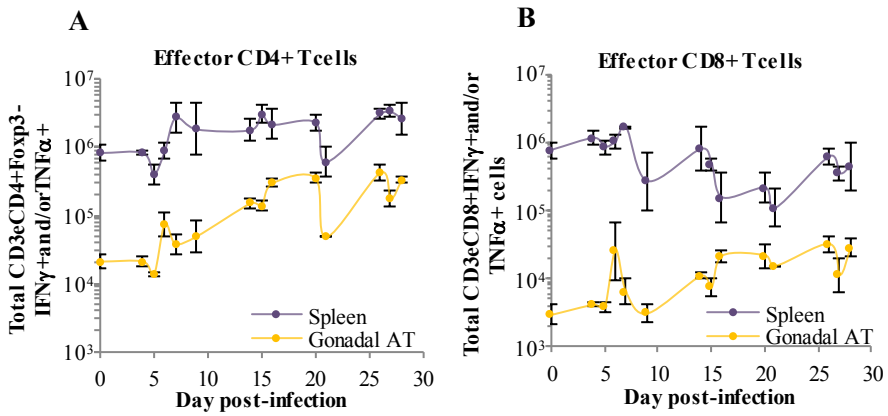

Supplementary figure 4. Dynamics of total effector CD4 T cells and effector CD8 T cells throughout infection. (A) Total number of effector CD4 T cells in spleen and gonadal AT **(B)** Total number of effector CD8 T cells in spleen and gonadal AT. **(A-B)** Error bars represent the standard error of the mean. (n=2-6 mice per group).

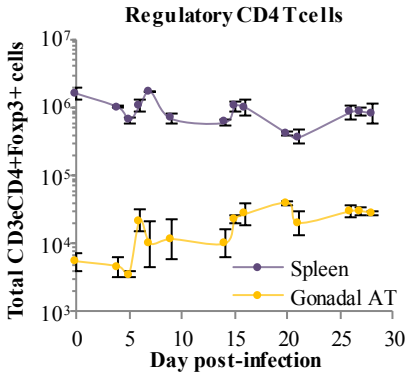

Supplementary figure 5. Dynamics of total regulatory CD4 T cells throughout infection. Total number of regulatory CD4 T cells in spleen and gonadal AT. Error bars represent the standard error of the mean (n=2-6 mice per group).

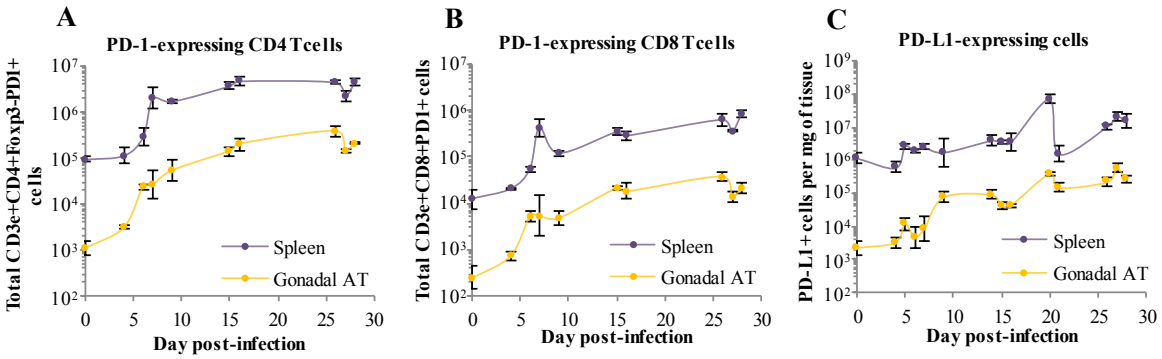

Supplementary figure 6. Dynamics of total PD-1-expressing CD4 T cells and CD8 T cells and total PD-L1-expressing cells throughout infection. (A) Total number of PD-1 expressing CD4 T cells in spleen and gonadal AT. **(B)** Total number of PD-1 expressing CD8 T cells in spleen and gonadal AT. **(C)** Total number of PD-L1 expressing cells in spleen and gonadal AT. **(A-C)** Error bars represent the standard error of the mean (n=2-6 mice per group).